



Review

Advances in Development of Radiometal Labeled Amino Acid-Based Compounds for Cancer Imaging and Diagnostics

Mária Bodnár Mikulová¹ and Peter Mikuš^{1,2,*}

¹ Department of Pharmaceutical Analysis and Nuclear Pharmacy, Faculty of Pharmacy, Comenius University in Bratislava, Odbojarov 10, 832 32 Bratislava, Slovakia; mikulova43@uniba.sk

² Toxicological and Antidoping Center (TAC), Faculty of Pharmacy, Comenius University in Bratislava, Odbojarov 10, 832 32 Bratislava, Slovakia

* Correspondence: mikus@fpharm.uniba.sk; Tel.: +421-2-501-17-243

Abstract: Radiolabeled biomolecules targeted at tumor-specific enzymes, receptors, and transporters in cancer cells represent an intensively investigated and promising class of molecular tools for the cancer diagnosis and therapy. High specificity of such biomolecules is a prerequisite for the treatment with a lower burden to normal cells and for the effective and targeted imaging and diagnosis. Undoubtedly, early detection is a key factor in efficient dealing with many severe tumor types. This review provides an overview and critical evaluation of novel approaches in the designing of target-specific probes labeled with metal radionuclides for the diagnosis of most common death-causing cancers, published mainly within the last three years. Advances are discussed such traditional peptide radiolabeling approaches, and click and nanoparticle chemistry. The progress of radiolabeled peptide based ligands as potential radiopharmaceuticals is illustrated via novel structure and application studies, showing how the molecular modifications reflect their binding selectivity to significant onco-receptors, toxicity, and, by that, practical utilization. The most impressive outputs in categories of newly developed structures, as well as imaging and diagnosis approaches, and the most intensively studied oncological diseases in this context, are emphasized in order to show future perspectives of radiometal labeled amino acid-based compounds in nuclear medicine.

Keywords: amino acid; peptide; bifunctional chelating agent (BFCA); radiolabeling; cancer; receptor; imaging



Citation: Mikulová, M.B.; Mikuš, P. Advances in Development of Radiometal Labeled Amino Acid-Based Compounds for Cancer Imaging and Diagnostics.

Pharmaceuticals **2021**, *14*, 167.
<https://doi.org/10.3390/ph14020167>

Academic Editor:
Daniela Montesarchio

Received: 12 January 2021
Accepted: 18 February 2021
Published: 21 February 2021

Publisher's Note: MDPI stays neutral with regard to jurisdictional claims in published maps and institutional affiliations.



Copyright: © 2021 by the authors. Licensee MDPI, Basel, Switzerland. This article is an open access article distributed under the terms and conditions of the Creative Commons Attribution (CC BY) license (<https://creativecommons.org/licenses/by/4.0/>).

1. Introduction

Over past 20 years, in the field of nuclear medicine, substantial progress has been made in the development of novel radiopharmaceuticals and radiolabeled agents for diagnosis and therapy of various diseases. Nowadays, a great emphasis is put on a synthesis and study of radiolabeled amino acid-derived biomolecules with a selective distribution and binding to target structures in living cells and tissues, i.e., enzymes, transporters, or peptide receptors. This allows targeted therapy and diagnostic evaluation of pathological changes in many fields, such as oncology, neurology, endocrinology, cardiology, and also investigation of inflammation processes or infection.

Especially, malignant tumor diseases are of the biggest interest because of their increasing global incidence, and placing second in the causes of death. The effect of target-specific radiolabeled compounds is often mediated through binding with high affinity to specific protein structures (e.g., active places in enzymes or receptors). Many of these structures are overexpressed in diseased cells compared to their absence or lower density under physiological conditions. Since that, such radiolabeled compounds represent effective probes in a recognizing and visualizing tumor cells in their early stage. All types of malignant solid tumors often exhibit lower oxygenation levels than their original tissues resulting in a hypoxic state, which impacts on the reduced effectiveness of tumor therapy and propagation of metastasis. Hence, there is an urgent need to enhance detection approaches for

monitoring various tumor types, including hypoxic cancer lesions. In this field, amino acid-based target-specific radiopharmaceuticals have become significant tools in modern oncology allowing cancer imaging on molecular and cellular level [1].

In order to utilize biomolecules for imaging and diagnosis, they must be properly labeled. Metal radionuclides belong to the most powerful and the most employed labels in nuclear medicine. In the group of metallic radioisotopes, gamma and positron emitters, namely copper-62, copper-64, gallium-67, gallium-68, indium-111, and technetium-99m have proved to be the most suitable for nuclear research and clinical application [2,3]. Apparently, other potential radionuclides such as zirconium-89, yttrium-86, and cobalt-55 have been included in recent studies since these have become more readily available with high purity. A diversity of synthesis strategies, radiolabeling approaches, modified chelators, and linkers has been investigated and developed to reach the optimized target-specific radiolabeled compounds, with proper characteristics for cancer imaging and therapy. All of these crucial components of radiolabeled compounds are the subject of many review papers, with a focus on the chemistry of metallic radionuclides [4–6], chelators, and linkers [7–12], as well as onco-specific peptidic biomolecules [2,13–16].

The aim of this review is to summarize and critically evaluate state-of-the-art approaches and the most significant outputs related to the development of target-specific radiometal labeled biomolecules for imaging of severe tumor types and tumors with an increased incidence. Recent advances in synthetic approaches and radiometal-labeling strategies of amino acid-based biologically active molecules, including most employed peptide families and receptors such as somatostatin, cholecystokinin/gastrin, bombesin, integrins, and hypoxia endogenous markers, as well as inhibitors of prostate-specific membrane antigen and fibroblast activation protein, are highlighted in order to demonstrate perspectives in cancer diagnostics with amino acid-based radiopharmaceuticals.

2. Basic Characteristics of Conventional Metal Radionuclides and Chelators Currently Used in Nuclear Medicine

Radiometallic compounds with targeted biodistribution and binding in the human body (i.e., target-specific) include in their structure: (i) biomolecules as a crucial biodistribution component (specific to receptor); (ii) a linker as a connecting component preserving specificity of biomolecule when attaching; (iii) a bifunctional chelating agent (BFCA); and (iv) metal radionuclides (see Figure 1). Basic characteristics of the most important or most frequently used representatives in the group of conventional metal radionuclides and BFCA are briefly discussed in Sections 2.1 and 2.2, respectively. Discussion is led in general point of view or, if appropriate, with respect to amino acid based biomolecules.

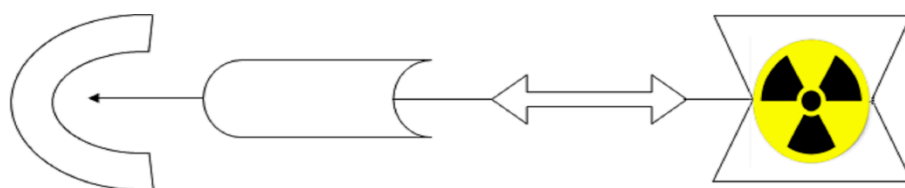


Figure 1. Basic scheme of a potential target-specific radiopharmaceutical.

2.1. Metal Radionuclides

In general, a diagnostic radioprobe contains a gamma emitting radionuclide for SPECT imaging or a positron emitting radionuclide for PET imaging. Basic parameters of the most common metallic radionuclides for diagnostic nuclear medicine are summarized in Table 1.

Nuclear medicine research is currently focused on development of a highly potent target-specific biomolecule labeled with positron emitters (predominantly gallium-68, but also zirconium-89, copper-64, and others). Anyway, there is still a leading position of technetium-99m in diagnostic clinical practice. In research, a prognosis for the development of Tc-radiopharmaceuticals is also quite positive due to novel modifications of BFCA and linkers continuously presented and developed for SPECT imaging.

Table 1. Selected metallic radionuclides employed in diagnostic nuclear medicine.

Isotope	Radiation Type	E _{max} [keV] (Decay %)	Half-Life	Production (Common Reaction)	Main Application Areas
^{99m} Tc	γ	141 (89.1%)	6.01 h	⁹⁹ Mo/ ^{99m} Tc generator (cyclotron alternatively)	SPECT of lung, brain, myocard, bones, kidney, liver, etc.
¹¹¹ In		171.3 (90.2%) 245.4 (94%)	2.83 d	cyclotron, ¹¹² Cd(p, 2n) ¹¹¹ In	SPECT of somatostatin receptor-positive NET
⁶⁷ Ga		93.3 (37%), 184.6 (20.4%), 300.2 (16.6%)	3.26 d	cyclotron, ⁶⁸ Zn(p, 2n) ⁶⁷ Ga	scintigraphy of inflammation, infection, tumors
⁶⁴ Cu	β ⁺	653 (17.6%)	12.7 h	cyclotron, ⁶⁴ Ni(p, n) ⁶⁴ Cu	PET imaging of hypoxic tumors, integrin- and gastrin-releasing peptide receptor-positive tumors
⁶⁸ Ga		836 (89%)	67.7 m	⁶⁸ Ge/ ⁶⁸ Ga generator (cyclotron alternatively)	PET imaging of somatostatin receptor-, PSMA-, FAP-overexpressed tumors
⁸⁹ Zr		395 (23%)	3.3 d	cyclotron, ⁸⁹ Y(p, n) ⁸⁹ Zr	immuno-PET imaging

Dosimetry and imaging aspects, depending on a particular radiolabeled compound and its properties, as well as an overall condition of a patient, can be found (if they were evaluated) in individual imaging studies discussed in Section 4.

2.2. Bifunctional Chelating Agents (BFCA)

Since the metallic radionuclides themselves cannot be utilized in a direct radiolabeling of amino acid-based target-specific compounds (peptides, proteins), it is necessary to develop bifunctional chelating agents (BFCA) [12]. An appropriate BFCA can properly attach both a metallic radionuclide and a biomolecule as well. The double function of BFCA helps the biomolecule to retain its receptor specificity and, thus, to match metal properties with the intended utilization in the imaging/therapy of various diseases. The choice of BFCA takes into account the oxidation state and nature of the metallic radionuclide. The optimal BFCA should provide thermodynamically stable and kinetically inert complexes, rapid reaction (at low temperatures and concentration), flexible conjugation chemistry, and should be easily accessible [17,18].

Various acyclic and cyclic BFCA have been introduced into (potential) radiopharmaceuticals. Traditional examples of acyclic and cyclic BFCA are discussed in Sections 2.2.1 and 2.2.2, respectively, while the most commonly used BFCA in radiolabeling with a particular diagnostic radiometal including newer developed chelators in Sections 3.2.1–3.2.5.

2.2.1. Acyclic BFCA

The polyaminopolycarboxylic acids-derived BFCA, such as DTPA, EDDA, EDTA, as well as tripeptide MAG3 (Figure 2), are the most commonly used acyclic BFCA containing hard donor atoms (N, O) in their molecule to form the coordination bond with metallic radionuclide. Another acyclic chelator, a siderophore-based desferrioxamine-B (DFO) has been utilized for effective radiolabeling of biomolecules with a metal. The thermodynamic stability and inert kinetics of a formed complex is unique and influenced by properties of both, a metal radionuclide as well as a BFCA. A significant advantage of the acyclic BFCA is faster metal binding kinetics, resulting in a faster radiolabeling procedure [17]. On the contrary, acyclic BFCA form less stable complexes than cyclic ones due to a higher interaction probability and more fixed geometry of donor atoms in the cyclic BFCA [18].

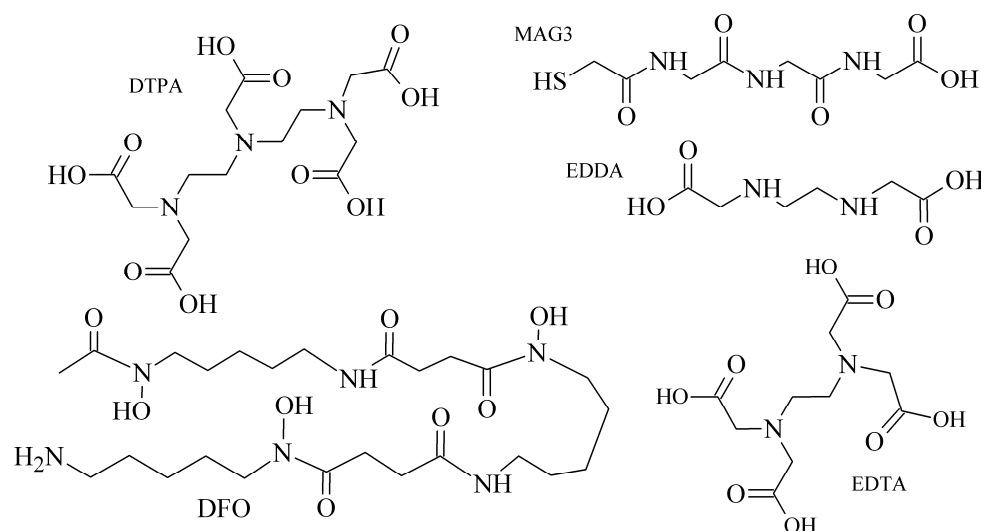


Figure 2. Chemical structures of the most common acyclic chelators as a base of BFCA.

2.2.2. Cyclic BFCA

The cyclic BFCA containing macrocycle such as DOTA, NOTA, TETA, and their derivatives as well as various structurally related analogues (for selected representatives see Figure 3) are holding an important position in syntheses of radiolabeled peptide-based compounds over a long period. Several new next generation cyclic chelators or chelators derived from traditional ones with improved properties have been developed over past decade such as PCTA, AAZTA, TRAP, THP, and fusarinine C [19]. As mentioned above, cyclic BFCA are beneficial generally by providing more kinetically inert and thermodynamically stable complexes with metal radionuclides. In order to obtain complexes with enhanced stability, several properties have to be considered such as hard and soft acid and base concept, a higher number of donor atoms providing a better steric fixation of complex, and a proper cavity size for the encapsulation of the whole size of metal ion in a tight structural arrangement.

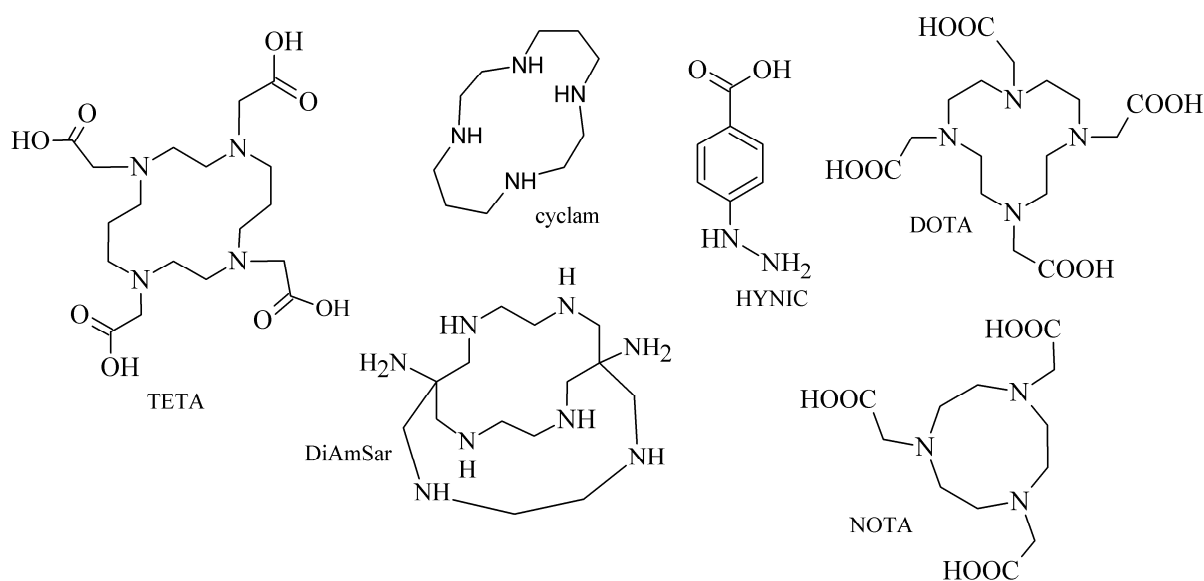


Figure 3. Chemical structures of the most common cyclic chelators as a base of BFCA.

DOTA is considered as the golden standard of chelators owing to its high kinetic stability. Several types of DOTA-derived chelators have been developed to bind with target peptide biomolecules, i.e., protected DOTA forms, active DOTA esters, and DOTA- deriva-

tives with a coupling moiety [20]. Concerning NOTA, derivatives with aminocarboxylic acids have been applied as BFCA, e.g., NODAGA (with glutaric acid), NODASA (with succinic acid), or NODAPA (with *p*-phenylacetic acid) [21]. Abrams and co-workers used 6-hydrazinopyridin-3-carboxylic acid, in short HYNIC, for radiolabeling of a polyclonal antibody with technetium-99m [22]. Ever since, HYNIC has become the most convenient chelator for ^{99m}Tc -labeled peptides and antibodies. Other chelators related to bsthiosemicarbazone [23,24], cyclam [25,26], and sarcophagine [27,28] have been increasingly studied to improve kinetic inertness and stability of complexes, especially those with copper isotopes.

3. Complexes and Radiolabeling Approaches for Target-Specific Peptide Molecules

The amino acids, main peptide and protein building blocks, play an important role essentially in all biological processes. Radiolabeled amino acids (AA) have become actively studied, owing to the role of their transporters in the tumor environment. Studies indicated that AA transporters, which recognize, bind and carry amino acids across the plasma membrane, serve not only to maintain nutritional requirements, but also to accumulate particular amino acids in specific cells [29,30].

Analogously, radiolabeled peptides as amino acid-based biomolecules are in the center of interest in the field of nuclear medicine and pharmacy because their biological action is mediated upon selective binding to specific peptide receptors and transporters overexpressed in numerous tumor cells. These receptors have shown potential as a molecular target for tumor imaging or targeted therapy with radiolabeled peptides (for the most important onco-specific peptide receptors and radiolabeled peptides see Section 4). The following Sections 3.2–3.4 are dealing with current radiolabeling approaches used for peptides and showing corresponding complex structures.

3.1. Peptides as Target-Specific Molecules and Their Synthesis

Peptides can be simply synthesized by a solid phase peptide synthesis (SPPS) [31,32] and modified to obtain optimized pharmacokinetic properties. The synthetic procedure can be carried out manually [33], e.g., in syringes, or automatically in commercial synthesizers [34]. A general pattern for the solid-phase peptide synthesis is depicted in Figure 4.

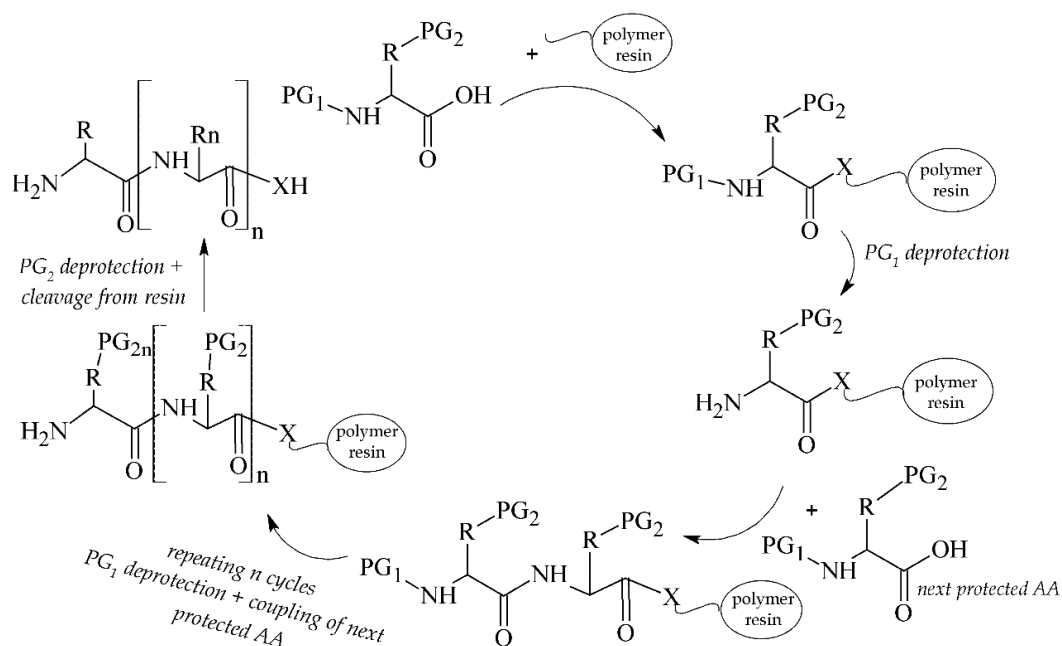


Figure 4. Scheme of solid phase peptide synthesis (SPPS). PG₁ = temporary protecting group; PG₂ = semi-permanent protecting group; X = N/O.

The advantages of peptides over proteins and antibodies can be seen in a preparation method, a rapid blood clearance, and the ability to tolerate harsh reaction conditions. On the other hand, a rapid enzymatic degradation by physiological peptidases is a significant limitation of peptides. Anyway, there are several strategies how to avoid this drawback including structural modifications of the C-/N-terminus, incorporation of a PEG linker or D-/unnatural AA, and cyclization [35].

3.2. Conventional Radiolabeling Approaches of Peptides with Metallic Radionuclide

The choice of a radiolabeling approach depends on radionuclide nature and a bioactive molecule. A direct labeling strategy is more difficult to be used for a metal attachment to biomolecules (e.g., peptides, proteins). Since the direct approach provides low site-specific and unstable products, and is applicable only to antibodies and their fragments, an indirect labeling method with BFCA has become preferred for a metal-peptide linkage. The usage of BFCA often requires multistep synthesis and involves non-specific interactions, thus a searching for new strategies with more effective incorporation of BFCA into peptide biomolecules has led to innovative approaches in the radiochemistry field such as click reactions (Section 3.3) and radiolabeled nanoparticles (Section 3.4). Modified BFCA and linkers may improve pharmacokinetic properties of a radiolabeled compound. Conventional radiolabeling approaches and chemical structures of corresponding complexes with the most frequently used metal diagnostic radionuclides are discussed in following Sections 3.2.1–3.2.5.

3.2.1. Radiolabeling of Peptide-Based Compounds with Technetium-99m

Technetium-99m has been the most frequently used radionuclide in nuclear medicine since the $^{99}\text{Mo}/^{99\text{m}}\text{Tc}$ generator development in 1957. Indirect labeling approaches, such as pre-labeling (labeling before conjugation with biomolecule) or post-labeling (labeling after conjugation with biomolecule), are of the routine for $^{99\text{m}}\text{Tc}$ -coordination. The pre-labeling procedure (Figure 5) is very useful in research to prove the concept and define the chemistry, contrary to a clinical use because of a long lasting radiosynthesis and hardly accomplished kit formulation [3].

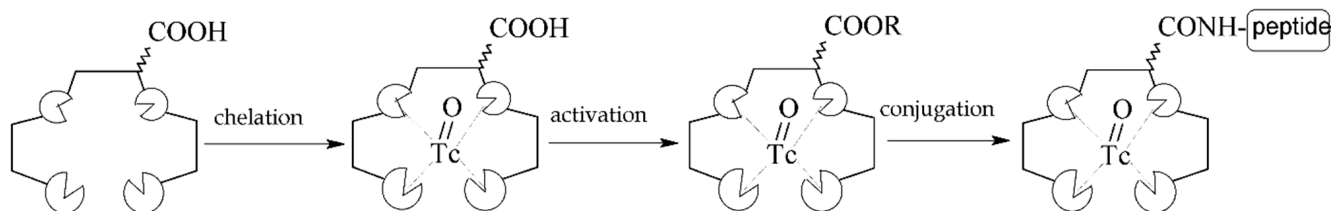


Figure 5. Scheme of the pre-labeling procedure with technetium-99m (adapted according to [3]).

The post-labeling procedure (Figure 6) is the most widely used for a synthesis of target-specific peptide radiopharmaceuticals.

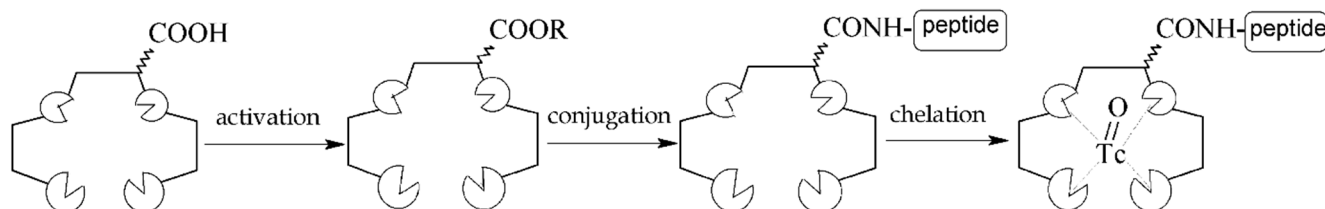
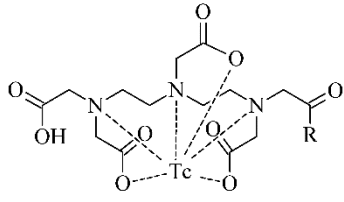
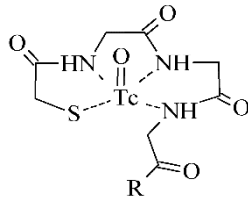
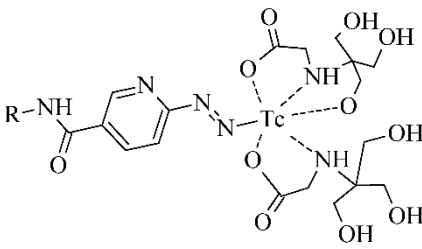


Figure 6. Scheme of the post-labeling procedure with technetium-99m (adapted according to [3]).

Technetium chemistry, its cores and complexes, have been thoroughly reviewed in recent years [4,6,36,37]. The most frequently studied BFCA for Tc-complexes are summarized in Table 2. In past few years, $^{99\text{m}}\text{Tc}$ -Tc-HYNIC has been the most commonly used core for the conventional radiolabeling of bioactive peptides for tumor imaging such as RGD

peptides [38,39], α -MSH peptide analogues [40,41], bombesin analogues [42,43], substance P analogues [44], or glucagon-like peptide analogues [45].

Table 2. The most common BFCA for ^{99m}Tc -labeled compounds.

BFCA	Complex Structure	References
DTPA and its derivatives		[46]
MAG3		[47]
HYNIC (with tricine coligand)		[48]

3.2.2. Radiolabeling of Peptide-Based Compounds with Gallium-68

Gallium is represented by the oxidation state III+ in aqueous solution and acts as a hard Lewis acid. It binds to hard Lewis bases such as nitrogen and oxygen donor groups of carboxylates, hydroxamates, amines [17]. It can be relatively easily hydrolyzed at pH 4–7 [49]. Gallium forms complexes with the maximum coordination number of 6 in a pseudo octahedral geometry, but four- or five-coordinate complexes are also formed [17,49]. For a ^{68}Ga -labeling procedure, well-known representatives and the most frequently used BFCA are derived from 1,4,7-triazacyclononane and 1,4,7,10-tetraazacyclododecane, e.g., DOTA and NOTA, including their recently developed derivatives such as TRAP, PCTA, NOTP, and THP and DATA, among others (see examples in Table 3).

Table 3. The most common BFCA for ^{68}Ga -labeled compounds.

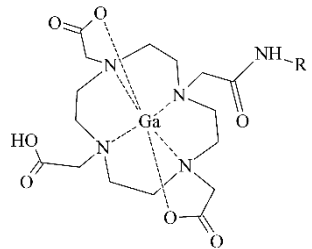
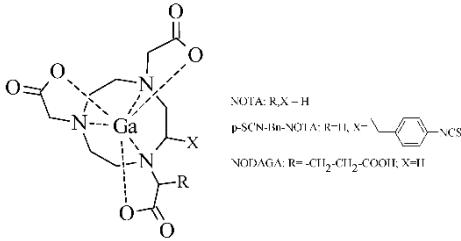
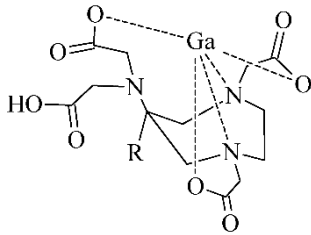
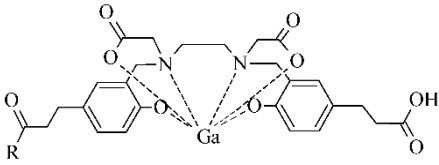
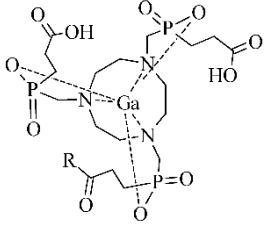
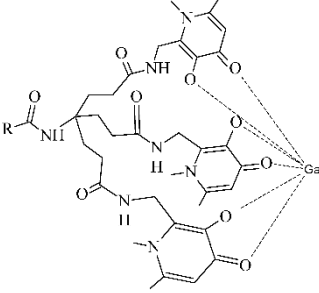
BFCA	Complex Structure	References
DOTA and its derivatives		[21,50,51]

Table 3. Cont.

BFCA	Complex Structure	References
NOTA and its derivatives		[52]
AAZTA and its derivatives		[53]
HBED-CC		[54,55]
PrP9 and its derivatives		[56]
THP and its derivatives		[57]

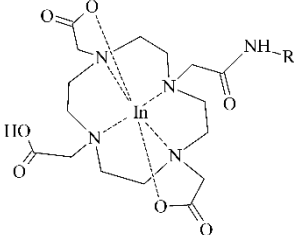
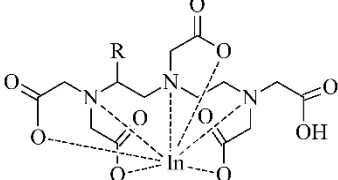
The ^{68}Ga -labeled biomolecules have been studied for somatostatin receptor-positive tumor imaging over a long period [58–60] with several highly potent agents in clinical trials or one already approved. Current studies with gallium-68 have followed up various malignancies with prostate-specific membrane antigen (PSMA) and fibroblast activation protein (FAP) [55,61,62].

3.2.3. Radiolabeling of Peptide-Based Compounds with Indium-111

Indium-111 has several properties for coordination chemistry with gallium-68 in common. The only stable oxidation state of indium-111 is III+ and acts as the Lewis acid, but softer donor groups can be offered to create seven or eight-coordinated complexes [49]. The ionic radius of indium-111 (0.92 Å) is significantly larger than that of gallium-68 (0.65 Å) what results in different coordination in macrocycles. The DTPA- and DOTA-based

chelators usually in *t*-butyl forms are generally the most employed for the ^{111}In -labeling (see Table 4) [63].

Table 4. The most common BFCA for ^{111}In -labeled compounds.

BFCA	Complex Structure	References
DOTA and its derivatives		[64,65]
DTPA and its derivatives		[66]

Studies covering ^{111}In -labeled biomolecules are aimed at somatostatin receptor imaging [66], glucagon-like peptide receptor [67,68], gastrin-releasing peptide receptor [69], or integrins [70].

3.2.4. Radiolabeling of Peptide-Based Compounds with Copper-64

The most stable oxidation state of copper in aqueous solution is $\text{II}+$ creating complexes with donor atoms such as amine-, imine- and pyridine-N, carboxylate-O, and thiol-S [17]. Although the copper chelation chemistry has been thoroughly reviewed [13,18,49,71], there is still a challenge in the development of *in vivo* stable Cu-BFCA complexes due to labile character of Cu(II) . The design of copper radiopharmaceuticals has put emphasis on polyaza-macrocycles derived BFCA (see Table 5). Due to only moderate stability of ^{64}Cu -DOTA-labeled biomolecules under *in vivo* conditions and high liver accumulation, a number of cross-bridged cyclam derivatives were developed to form more stable ^{64}Cu -complexes [25,26,72].

^{64}Cu -labeled compounds have been included, mostly in the studies of tumors with overexpressed gastrin-releasing peptide [73,74] and $\alpha_v\beta_3$ integrin receptors [75,76], and prostate-specific membrane antigen [77].

Table 5. The most common BFCA for ^{64}Cu -labeled compounds.

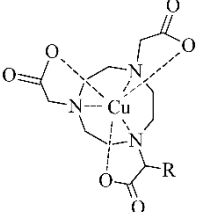
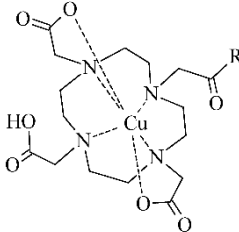
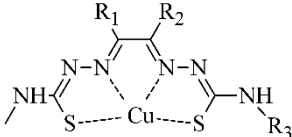
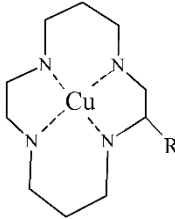
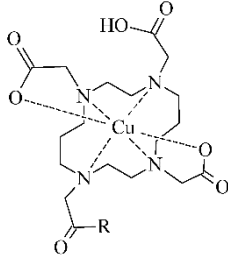
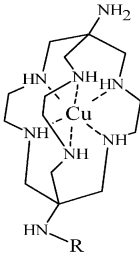
BFCA	Complex Structure	References
NOTA and its derivatives		[78,79]

Table 5. Cont.

BFCA	Complex Structure	References
DOTA and its derivatives		[80]
bisthiosemicarbazones		[24,81,82]
cyclam		[26]
TETA and its derivatives		[83,84]
sarcophagines		[28,85]

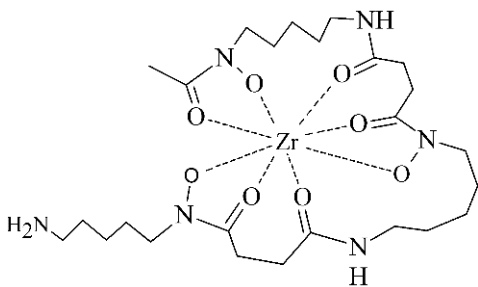
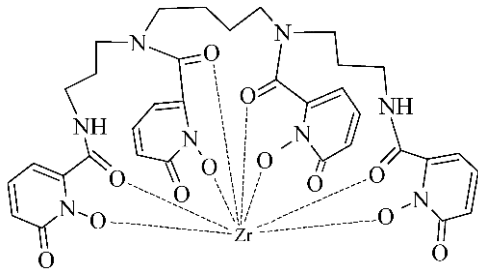
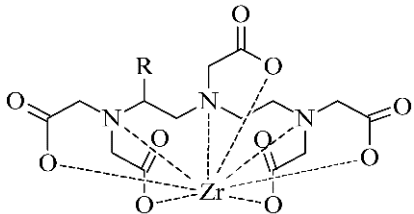
3.2.5. Radiolabeling of Peptide-Based Compounds with Zirconium-89

Zirconium is a metal belonging to the group IV that exists primarily in +IV oxidation state in aqueous media. This cation is relatively large, acts as the hard Lewis acid and prefers anionic oxygen donor groups to create complexes with high coordination number [86]. Depending on pH, oxides and hydroxides of zirconium form polynuclear species upon hydrolysis at very low pH and mononuclear hydrolysis species at pH between 0 and 2 [87].

In order to effectively utilize zirconium-89, various chelators have been employed such as DOTA, DTPA, as well as the most successful desferrioxamine B and 3-hydroxypyridin-2-one (2,3-HOPO) derivatives (see Table 6).

Zirconium-89 has been applied mostly in labeling of monoclonal antibodies for PET imaging of immune-based strategies [88], but there has been a progress in the design of ⁸⁹Zr-labeled small peptide PSMA-inhibitors for prostate cancer imaging lately [89].

Table 6. The most common BFCA for ^{89}Zr -labeled compounds.

BFCA	Complex Structure	References
DFO and its derivatives		[89]
2,3-HOPO and its derivatives		[90]
DTPA and its derivatives		[91]

3.3. Radiolabeling Approaches of Peptides with Metallic Radionuclide Based on Click-Chemistry

Since Kolb et al. described “click reactions” in 2001 [92], this new chemistry has become rapidly growing in various chemical fields and, since 2006, also in the radiochemistry field. There are two main characteristics making the click chemistry attractive, i.e., the bioorthogonality of reactions and mild reaction conditions (usually at room temperature and in aqueous media) [93]. Additional benefits include the selectivity, rapidity, and modularity of click ligations. The most associated term with the “click chemistry” is the Cu(I)-catalyzed azide-alkyne cycloaddition (CuAAC) forming 1,4-disubstituted 1,2,3-triazoles (see Figure 7A). Mindt et al. developed and extended the “click-to-chelate” methodology for radiometallic ligation [94,95], in which 1,2,3-triazole is an integral part of the chelating system. This approach has been successfully applied for Tc- and Re-tricarbonyl compounds, when tridentate ligands are coordinated to $\text{M}(\text{CO})_3$ core resulting in better pharmacokinetic properties [94,95].

In recent years, several catalyst-free site-specific reactions have been investigated for effective radiolabeling of peptide biomolecules and nanomaterials including tetrazines and trans-alkenes for the inverse electron-demand Diels–Alder reaction (IEDDA), azide and cyclooctyne functionalities for the strain-promoted azide-alkyne cycloaddition (SPAAC), and functionalized phosphanes for the Staudinger ligation (Figure 7B–D) [8,96,97]

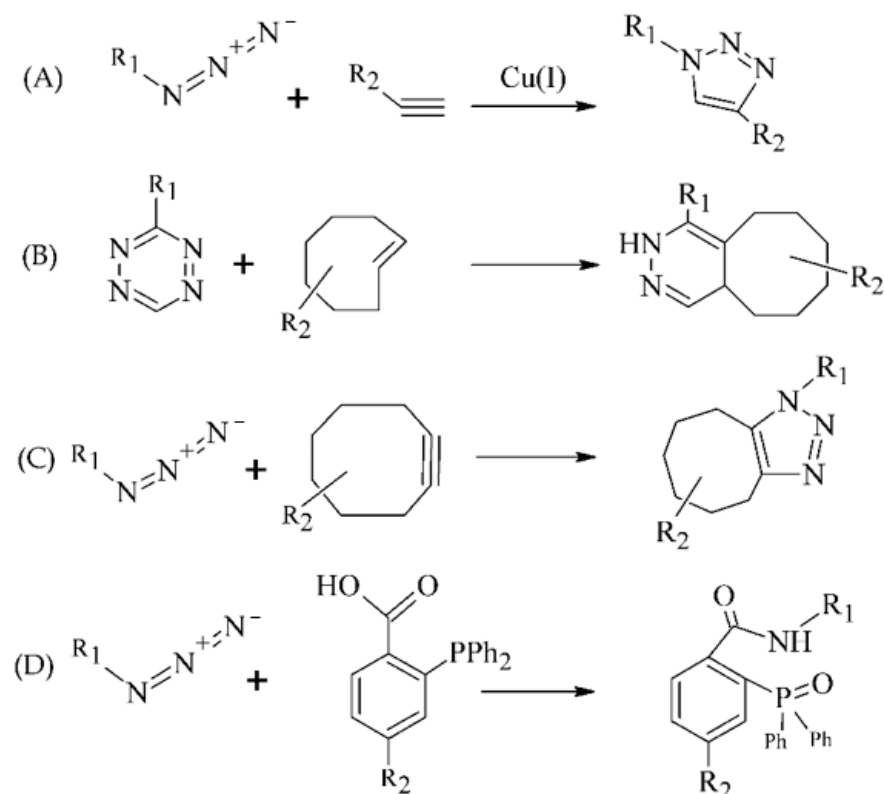


Figure 7. Selected click reactions for the preparation of intermediates used for metal chelating (R_1 , R_2 —proper chelating and peptide moieties). (A) CuAAC, (B) IEDDA, (C) SPAAC, (D) Staudinger ligation.

Within the “click-to-chelate” methodology, the development of new clickable chelators is currently attracting a growing interest (see examples in Figure 8). New clickable chelators have been designed for ^{99m}Tc -labeled peptides to obtain an increased hydrophilicity and decreased hepatobiliary retention of $([^{99m}\text{Tc}]\text{Tc}(\text{CO})_3)$ -complexes. Novel dipicolylamine derivatives, substituted with carboxylates on the pyridyl rings, were synthesized and evaluated for *fac*- $[\text{Tc}/\text{Re}^I(\text{CO})_3]^+$ complexation with α -MSH peptide analogue [98]; a propargyl-substituted thiocarbamoylbenzimidine acting as a tetradentate ligand for a conjugation with $[\text{Re}/\text{Tc}^V\text{O}]^{3+}$ cores [99]; or 1,4-substituted pyridyl-1,2,3-triazole derivatives with pendent phenyl isothiocyanate groups [100].

For ^{68}Ga - and ^{64}Cu -labeled probes, standard BFCA have been modified using various prosthetic groups. The DOTA- and NOTA-based click chelators with aldehyde, alkyne, aminoxy, azide, maleimide, monofluorocyclooctyne, and thiol functionalities were developed using CuAAC or RIKEN click reaction [101–104]; or with azide and tetrazine prosthetic groups using SPAAC and IEDDA reactions [105]. The HBED-chelator was modified with two azide groups (HBED-NN) and both azide and carboxylic groups (HBED-NC) [106]. Novel cyclic hydroxamate siderophore-based BFCA were reported as promising BFCA for gallium-68 [107]. Baranyai et al. optimized a procedure for the conjugation of 1,4,7-triazacyclononane-1,4,7-tris(methylene(2-carboxyethylphosphonic acid)) chelator (TRAP) with peptides using CuAAC [108]. The TRAP conjugates showed kinetic inertness and suitability for ^{64}Cu - and ^{68}Ga -coordination [109,110].

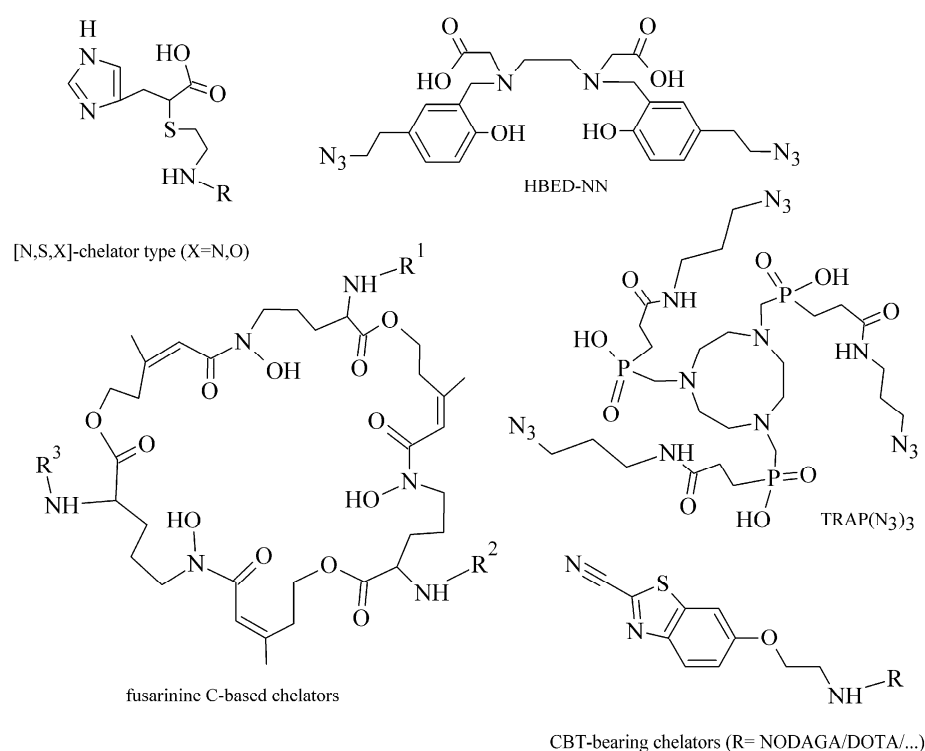


Figure 8. Examples of attractive clickable chelators for radiolabeling of biomolecules with metal radionuclides [106,108,111–113].

3.4. Radiolabeling Approaches of Peptides with Metallic Radionuclide Based on Nanoparticles

Nanomedicine has recently emerged as one of the most promising branches in medicine including a development of novel probes with improved properties for the site-specific detection or therapy of cancer. This rapidly growing trend is underlined by numerous reviews in the radiochemistry field [114–117]. Over past 10 years, tens of articles have been focused on the metal-labeled nanoparticles (NP) conjugated to various peptides for SPECT and PET cancer imaging (see a representative image of radiolabeled nanoparticles using electron microscopy in Figure 9).

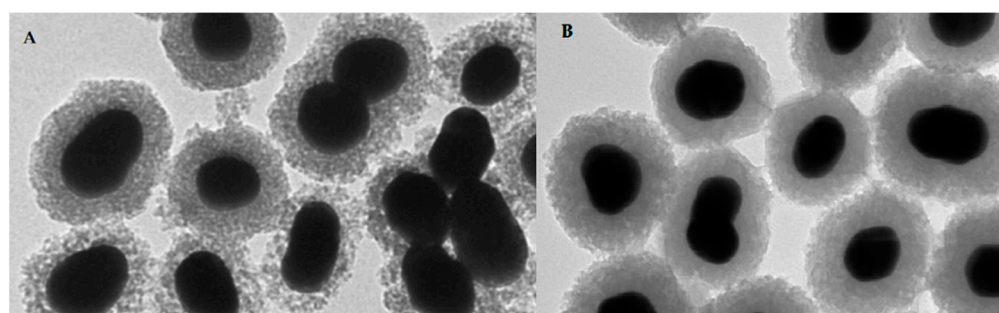


Figure 9. Representative image of PET-SERRS nanoparticles with non-optimized ⁶⁸Ga-labeling (A) with visible degradation of silica shells and after the optimization (B) with improved stability of the silica shells [118].

Radiolabeling of NPs with technetium-99m can be carried out by a direct or an indirect method. The direct approach is based on a reduction in [^{99m}Tc]TcO₄[−] with the acidic solution of stannous chloride followed by its direct binding and incorporation to a NP core. In the indirect method, BFCA is necessary to allow a stable linkage between radionuclide and NP [116]. The indirect method has been mostly used for the radiolabeling of ^{99m}Tc-NPs conjugated with peptides, see an illustrative example in Figure 10. Gold

NPs have been conjugated to peptides with [^{99m}Tc]Tc-HYNIC for integrin-positive glioma imaging [119], with [^{99m}Tc]Tc-DTPA for breast cancer imaging [120], for gastrin releasing peptide receptor imaging [121,122] and somatostatin receptor-positive neuroendocrine tumor imaging [123]. The NPs based on a polylactic acid polymer were conjugated to ^{99m}Tc -labeled octreotide for pancreatic polypeptide-secreting tumor imaging [124].

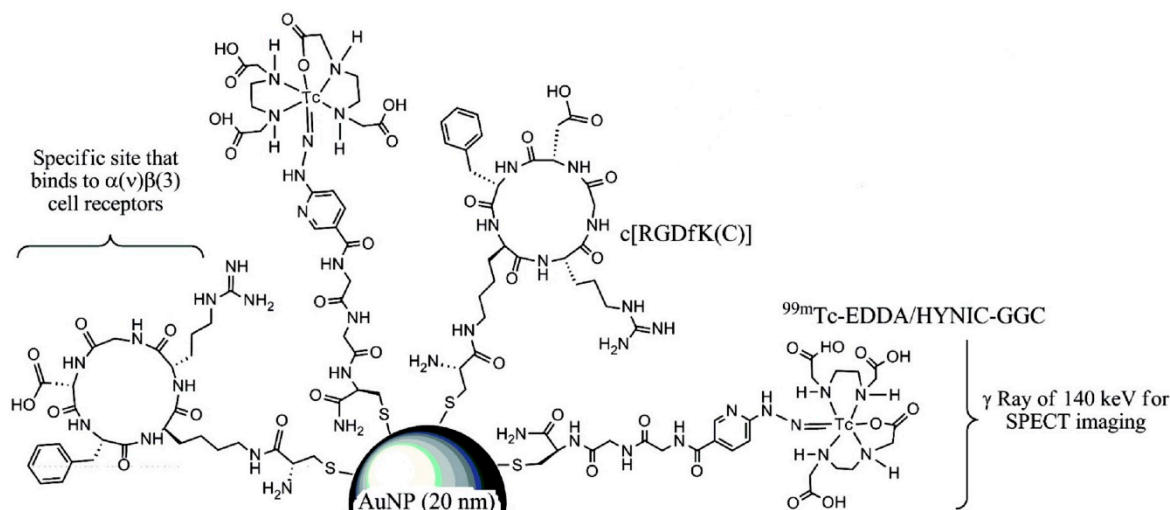


Figure 10. Illustrative scheme of [^{99m}Tc]Tc-EDDA/HYNIC-GGC conjugated to RGD derivative and gold NP [119].

Several published papers dealt with ^{111}In -labeled NPs conjugated to peptides such as directly labeled gold NPs for human melanoma and glioblastoma imaging [125], liposomal NPs conjugated to a RGD peptide analogue and the undecapeptide substance P for glioblastoma and melanoma targeting [126].

Furthermore, ^{64}Cu - and ^{68}Ga -labeled NPs functionalized with a peptide were reported in several papers too. The multifunctional gold nanorod nanocarriers were covalently bound with doxorubicin and subsequently conjugated to [^{64}Cu]Cu-NOTA-RGD [127]; [^{64}Cu]Cu-sulphide NPs conjugated to the pegylated bombesin [128]; [^{68}Ga]Ga-DOTA-somatostatin and neurotensin analogues to gold NPs [129]; [^{68}Ga]Ga-NODAGA-bombesin to the polyethylene glycol-coated ultra-small superparamagnetic iron-oxide nanoparticles [130]; and [^{68}Ga]Ga-DOTA-bombesin analogue conjugated to the *N,N,N*-trimethyl chitosan-coated magnetic nanoparticles for a breast cancer detection [131].

4. Onco-Receptors and Their Target-Specific Radiometal Labeled Peptide Molecules for Tumor Imaging

In the following Sections 4.1–4.6, the most commonly studied onco-receptors are summarized, briefly characterized (location and purpose in human body), and discussed in relation to the development and improvements in their significant radiometal labeled ligands and tumor imaging. In a similar way, radiometal labeled peptide inhibitors of tumor-related proteins (Section 4.7) and sulfonamide-based analogues for tumor hypoxia imaging (Section 4.8) are discussed. In the accompanied tables, examples of particular radiolabeled analogues along with corresponding onco-receptors used in a positive tumor imaging over past three years, advantages and limitations of the studied diagnostic systems are critically evaluated. An illustrative example of a study of radiolabeled [^{68}Ga]Ga-OPS202 and [^{68}Ga]Ga-DOTATOC biomolecules for NET imaging is in Figure 11.

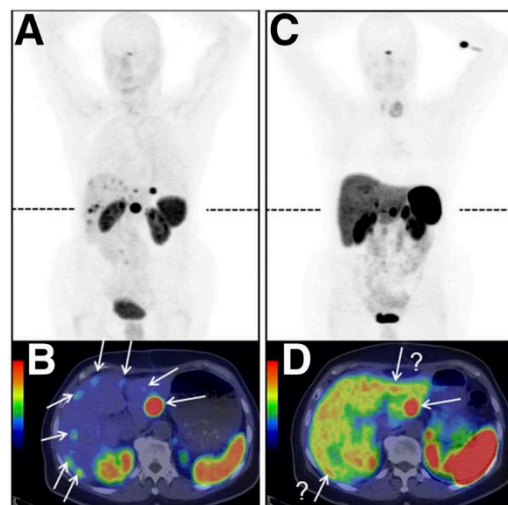


Figure 11. PET/CT images of a patient with ileal neuroendocrine tumors showing bilobar liver metastases (marked with arrows) after application of [^{68}Ga]Ga-OPS202 (A) and its transaxial fusion image (B) and [^{68}Ga]Ga-DOTATOC (C) and its transaxial fusion image (D) (adapted from [60]).

4.1. Somatostatin and Its Analogues for Somatostatin Receptors (SSTR) Imaging

Somatostatin (SST) is a physiological hormone occurring in two biologically active forms with the AA sequences illustrated in Figure 12. It regulates an endocrine and exocrine secretion throughout a human body.

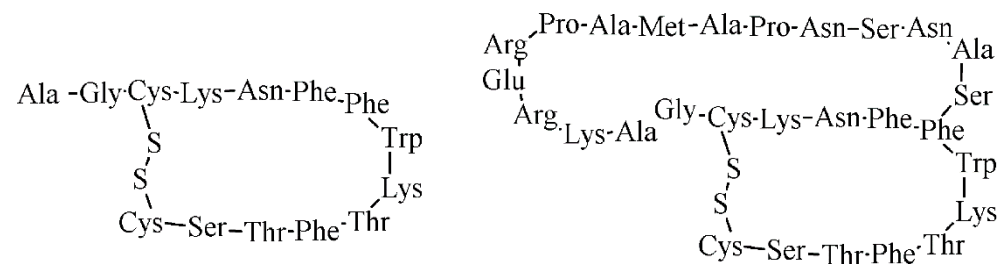


Figure 12. The AA sequence of two biologically active forms of somatostatin.

The biological effects of SST are mediated via 5 types of somatostatin receptors (SSTR) belonging to a G-protein coupled receptors family. SST, its analogues and receptors, have become increasingly popular and widely studied because of anti-tumor effects and mechanisms, including GEP-NETs [132], pituitary adenomas [133], breast cancer [134], small-cell lung cancer [135], melanoma [136], etc. The most commonly expressed receptor subtype in tumor cells is SSTR2, followed by SSTR1, SSTR5, SSTR3, and SSTR4 as the least expressed subtype [137]. Due to short biological half-lives of the natural SST, various synthetic analogues have been designed and evaluated to obtain more stable compounds (see Table 7). It can be stated, based on the examined published papers, there is a great effort to modify the DOTA-octreotide structure in order to achieve novel SST analogues with even better pharmacokinetic properties and specificity to avoid an intense uptake in liver, spleen, and kidney. The SST analogues labeled with gallium-68 and DOTA currently represent the best procedure for GEP-NET imaging. This statement is supported with a large number of research articles that include [^{68}Ga]Ga-DOTANOC, DOTATATE, and DOTATOC, respectively, for imaging of various tumors, such as head and neck paraganglioma [138]; pituitary adenoma and meningioma [139]; thyroid [140] and lung [141] carcinoma; and tumors in gastrointestinal system [60] as well. According to available literature from 2010, new approaches for syntheses of the SSTR-ligands seem to be not so extent, but since then, many consecutive examinations and reports have already been comprised of proven ligands for a variety of GEP-NET imaging in clinical trials.

Table 7. Summary of radiolabeled somatostatin analogues for SSTR-positive tumor imaging over past 3 years.

Composition of Studied Compounds - Metal Radionuclide - BFCA - Linker - Peptide	Results and Findings - Phase of Trials - Cancer Type Studied - Imaging Technique Used - Benefits/Limitations/Conclusion	Reference
- ⁶⁸ Ga - DOTA - x - TOC, TATE	- clinical, 10 patients - metastatic NET - PET, PET/CT - reduced signal from the liver achieved; methodology improvement needed for implementation of parametric-based kinetic analysis	[142]
- ^{99m} Tc, ¹⁷⁷ Lu - DOTA, HYNIC, EDDA -6-carboxy-1,4,8,11-tetraazaundecane (N4) -p-Cl-Phe-cyclo(D-Cys-Tyr-D-Trp-Lys-Thr-Cys)D-Tyr-NH ₂	- preclinical in vitro, in vivo - kidneys - SPECT/CT - more useful biodistribution results for a highly potent [^{99m} Tc]Tc-N4-conjugate than with lutetium-177; HYNIC-conjugate with complete loss of SSTR-2 affinity	[143]
- ⁶⁸ Ga - DOTA, NODAGA - x - JR11, TOC	- clinical, 12 patients - GEP-NET - PET/CT - very high TBR and image contrast of liver lesions for [⁶⁸ Ga]Ga-NODAGA-JR11; studies in larger patient group proven	[60]
- ⁶⁸ Ga - DOTA, fluorescein isothiocyanate - x - PA1, TATE	- preclinical in vitro, in vivo - lung, colorectal and gastric - microPET - effective tumor targeting and lower kidney accumulation of [⁶⁸ Ga]Ga-DOTA-PA1; a potential for PET/CT of SSTR-positive tumors (especially lung) suggested	[144]
- ⁶⁴ Cu - NODAGA, DOTA - x - JR11, TATE	- preclinical in vitro, in vivo - kidneys - microPET - more favorable in vivo pharmacokinetics, low levels in the liver, spleen and rapid blood clearance for [⁶⁴ Cu]Cu-NODAGA-JR11 with further development for clinical translation	[145]
- ^{99m} Tc - HYNIC, EDDA, tricine - x - TATE	- preclinical in vitro, in vivo; clinical, 6 patients - NET - SPECT/CT - reproducible kit with 2.96 GBq/6 mL formulated, but some differences in tumor uptake occurred	[146]
- ⁶⁸ Ga - DOTA - x - TOC	- clinical, 4 patients - GEP-NET - PET/MRI - sensitive and accurate evaluation of the liver, but limited accuracy of MRI related to lung and bone diseases	[147]
- ⁶⁸ Ga - DATA - x - TOC	- clinical, 53 patients - GEP-NET - PET/CT - comparable imaging profile of [⁶⁸ Ga]Ga-DATA-TOC with DOTA-NOC; DATA-conjugate useful for instant kit labeling	[148]

4.2. Bombesin and Its Analogues for Gastrin-Releasing Peptide Receptor (GRPR) Imaging

Bombesin (BBN) is a 14 AA peptide analogue (see the sequence in Figure 13) to the gastrin-releasing peptide and it represents an interesting probe for targeting of gastrin-releasing peptide receptors (GRPR) relevant in oncology.

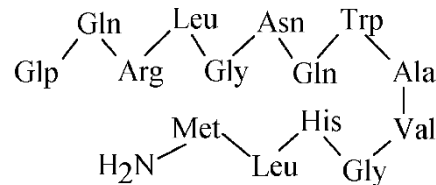


Figure 13. The AA sequence of bombesin peptide.

In total, four receptors belong to the family of GRPR, namely neuromedin B receptor BBR₁, gastrin-releasing peptide receptor BBR₂, orphan receptor BBR₃, and amphibious receptor BBR₄. Predominantly the BBR₂ is upregulated in cancer cells such as breast, lung, pancreas, colon, and prostate [149]. Research with radiolabeled BBN analogues has become increasing since the development of [^{99m}Tc]Tc-Lys³-BBN in 1998 [150]. Since then, most of these radiolabeled analogues have been designed as GRPR agonists with a favorable internalization in cancer cells. Meanwhile, several studies have demonstrated unwanted side effects of agonists connected with their GRPR activation, thus a research field has shifted its interest to antagonists [151]. Radiolabeled GRPR antagonists have shown superior value to the agonists in terms of better pharmacokinetic properties, very good in vivo stability and, by that, sufficient retention in cancer cells [152]. New GRPR antagonists have been developed with a potential for the clinical translations (see summarized studies in Table 8).

Table 8. Summary of radiolabeled bombesin analogues for GRPR-positive tumor imaging over past 3 years.

Composition of Studied Compounds	Results and Findings	Reference
- Metal Radionuclide	- Phase of Trials	
- BFCA	- Cancer Type Studied	
- Linker	- Imaging Technique Used	
- Peptide	- Benefits/Limitations/Conclusion	
- ⁶⁷ Ga, ⁶⁸ Ga, ¹¹¹ In, ¹⁷⁷ Lu - DOTA - <i>p</i> -aminomethylaniline-diglycolic acid - NeoBOMB1	- preclinical in vitro, in vivo; clinical, 4 patients - prostate - PET/CT - [⁶⁸ Ga]Ga-NeoBOMB1 with preserved GRPR affinity, high in vivo stability, and high contrast image in patients	[152]
- ⁵⁵ Co, ⁵⁷ Co - NOTA - PEG ₂ - RM26	- preclinical in vitro, in vivo - prostate - SPECT/CT, PET/CT - favorable pharmacokinetics and 3-fold lower internalization of ⁵⁵ Co-labeled peptide compared to ¹¹¹ In-labeled conjugate making it potential “next day” high contrast PET imaging probe	[153]
- ⁶⁴ Cu - DOTA with hydroxamic acid arms (DOTHA ₂), NOTA - PEG - RM26	- preclinical in vitro, in vivo - prostate - microPET/CT - fast elimination and slightly better in vivo imaging properties for DOTHA ₂ -conjugate than reference	[73]
- ⁶⁴ Cu - DOTA, NODAGA - [Pro-Gly] ₁₂ linker, PEG ₃ - RGD, BBN(7–14)	- preclinical in vitro, in vivo - prostate - microPET - NODAGA-conjugate for dual α _v β ₃ /GRPR targeting with better pharmacokinetics than DOTA, but low tumor uptake in vivo	[74]

Table 8. Cont.

Composition of Studied Compounds - Metal Radionuclide - BFCA - Linker - Peptide	Results and Findings - Phase of Trials - Cancer Type Studied - Imaging Technique Used - Benefits/Limitations/Conclusion	Reference
- ^{68}Ga - DOTA - <i>N</i> -(γ -maleimidobutyryloxy) succinimide ester - PSMA, Lys ³ -BBN(1-14)	- preclinical in vitro, in vivo - pulmonary and prostate - microPET/CT - higher cell uptake and internalization, greater affinity for GRPR but lower for PSMA of dimer compared to single [^{68}Ga]Ga-BBN/-PSMA monomers	[154]
- ^{68}Ga - DOTA -4-amino-1-carboxymethylpiperidine - RM2	- clinical, 16 patients - prostate - PET/CT, multiparametric MRI - fusion of MRI and PET/CT improved detection of a primary disease, but expression of GRPR and PSMA was not correlated	[155]
- ^{68}Ga - DOTA prepared from cyclen, DOTA-tris-(t-Bu) ester - x - BBN derivatives	- preclinical in vitro, in vivo - breast and prostate - preclinical nanoPET/CT - potency and efficiency of site-specific DOTA-cyclen comparable to that of DOTA-ester	[156]
- $^{99\text{m}}\text{Tc}$ - N4-chelator - PEG ₂₋₄ -D-Phe-Gln-Trp-Ala-Val-Gly-His-Leu-NH-CH ₂ -CH ₃	- preclinical in vitro, in vivo - prostate - gamma counter - PEG spacer length with only little effect on GRPR affinity, tumor uptake and in vivo stability	[157]
- $^{44\text{g}}\text{Sc}$, ^{68}Ga - DOTA - aminovaleric acid -Gln ⁷ -Trp ⁸ -Ala ⁹ -Val ¹⁰ -Sar ¹¹ -His ¹² -FA01010 ¹³ -Tle ¹⁴ -NH ₂	- preclinical in vitro, in vivo - prostate and breast cancer - PET/CT - $^{44\text{g}}\text{Sc}$ -conjugate with low uptake in breast cancer cells, but high tumor uptake and retention in prostate; differences in in vitro GRPR binding properties, but no in vivo	[158]

4.3. Cholecystokinin and Its Analogues for Cholecystokinin Receptor (CCKR) Imaging

Cholecystokinin (CCK) is a peptide hormone, which regulates various actions predominantly in the gastrointestinal tract and central nervous system. CCK was initially characterized with a 33 AA sequence, but later, the peptide was shown to be present in more biologically active forms (e.g., CCK4, CCK8, CCK33, CCK39) derived from a 115 AA precursor [159]. A total of three types of CCK receptors from the G-protein coupled receptors family have been identified, CCK1 known as CCK A, CCK2 known as CCK B, and CCK2i4sv receptor, respectively. The extensively studied receptors are CCK1, characterized in pancreatic cells and mainly located in periphery, and CCK2 located in the brain, stomach, pancreas, and gall bladder, and overexpressed in cancer types such as small cell lung cancers and medullary thyroid carcinomas [159]. The cholecystokinin octapeptide CCK8 (see its AA sequence in Figure 14) and minigastrin are of the most evaluated molecules for CCK2 receptors. All synthesized peptide analogues have the C-terminal receptor-binding tetrapeptide sequence of Trp-Met-Asp-Phe-NH₂ in common. Many of the CCK8 and minigastrin analogues were developed and evaluated up to 2010, the studies over past 3 years are summarized in Table 9.

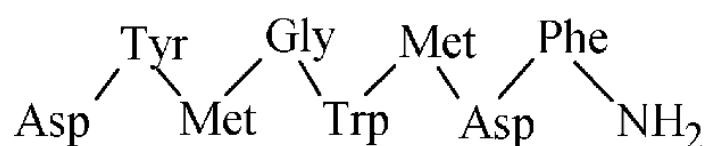


Figure 14. The AA sequence of octapeptide cholecystokinin.

Table 9. Summary of radiolabeled CCK/minigastrin analogues for CCKR-positive tumor imaging over past 3 years.

Composition of Studied Compounds - Metal Radionuclide - BFCA - Linker - Peptide	Results and Findings - Phase of Trials - Cancer Type Studied - Imaging Technique Used - Benefits/Limitations/Conclusion	Reference
- ^{68}Ga , ^{89}Zr - fusarinine C (FSC) - x -MG11	- preclinical in vitro, in vivo - epidermoid - microPET/CT - decreased hydrophilicity, increased metabolic stability and kidney retention for dimer and trimer, and reduced TBR of ^{89}Zr -monomer and dimers	[160]
- ^{111}In - DOTA - x - minigastrins MGS1, MGS2, MGS3, MGS4	- preclinical in vitro, in vivo - epidermoid, pancreatic - nanoSPECT/CT - modified C-terminal of [^{111}In]In-DOTA-MGS4 led to high CCK2R affinity, an improved biodistribution profile and a promising in vivo stability, tumor targeting, and TBR	[161]
- $^{99\text{m}}\text{Tc}$ - HYNIC, EDDA - x -MGS5, MGS11	- preclinical in vitro, in vivo - epidermoid - gamma counter, autoradiography - [$^{99\text{m}}\text{Tc}$]Tc-HYNIC-MGS11 with high resistance against enzymatic degradation and useful targeting profile similar to DOTA-analogue; a promising kit development of for CCK2R-imaging and radioguided surgery	[162]
- ^{111}In - DOTA - x - (D-Glu ¹⁻⁶)minigastrin	- clinical, 16 patients - advanced medullary thyroid - SPECT/CT - high uptake in lesions and favorable dosimetry confirmed, but increased calcitonin concentrations in blood; initiation of ^{177}Lu -analogue assessment	[163]

4.4. Exendin Analogues for Glucagon-Like Peptide 1 (GLP-1) Receptor Imaging

Glucagon-like peptide 1 (GLP-1) is an intestinal peptide hormone with a 36 AA sequence (see Figure 15), which stimulates insulin secretion. An action of the GLP-1 and its analogues is mediated through a glucagon-like peptide-1 receptor as a class B of G-protein-coupled receptor. The GLP-1 receptor was identified by radioligand binding experiments [164] and is expressed mainly in the stomach, pancreas, and brain. The GLP-1 receptor has been found predominantly in insulinomas, gastrinoma, pulmonary neuroendocrine tumors, and medullary thyroid cancer. GLP-1 analogues have been synthesized for the GLP-1 receptor targeting, from which exendin-4 as an agonist and exendin-3 as an antagonist have been widely studied (Table 10).

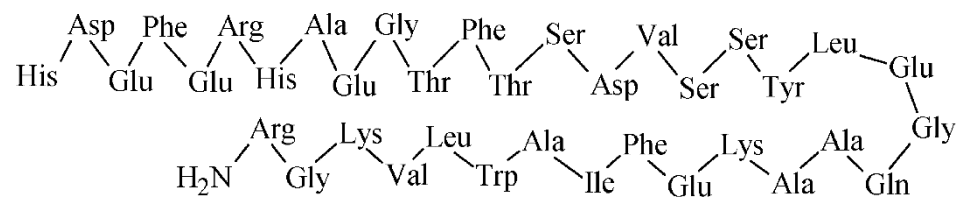


Figure 15. The AA sequence of GLP-1.

Table 10. Summary of radiolabeled exendin analogues for GLP-1 receptor-positive tumor imaging over past 3 years.

Composition of Studied Compounds - Metal Radionuclide - BFCA - Linker - Peptide	Results and Findings - Phase of Trials - Cancer Type Studied - Imaging Technique Used - Benefits/Limitations/Conclusion	Reference
- ^{111}In - DTPA - lysine - exendin-3	- preclinical in vitro, in vivo - insulinoma - SPECT - hexendin ^{40–45} conjugate (with 6 Lys and 6 DTPA residues) as the most useful due to the 7-fold higher specific activity than simpler conjugates and improved visualization of the pancreas	[67]
- ^{111}In - NODAGA - albumin-binding moiety (ABM) - exendin-4	- preclinical in vitro, in vivo - insulinoma - SPECT/CT - significantly reduced kidney uptake and improved GLP1R targeting, but a further assessment of whole-body doses needed	[68]
- ^{68}Ga - NOTA - methylaminolevulinate - Cys ³⁹ -exendin-4	- preclinical in vitro, in vivo - pheochromocytoma (PCM) - microPET - specific GLP1R targeting in both poorly and highly differentiated PCM cells, but high accumulation in kidneys; more studies needed to establish association between GLP-1R PET and a risk stratification of PCM	[165]
- ^{64}Cu - NODAGA x - Lys ⁴⁰ -exendin-4	- preclinical in vivo - insulinoma - PET/MRI - high background signal from the exocrine pancreas observed during an early time points; the positive correlation between [^{64}Cu]Cu-Ex4, reflecting β -cell mass, and Mn-retention demonstrated by a simultaneous PET/MRI	[166]

4.5. RGD Analogues for Integrin Receptors Imaging

Nowadays, over 20 subtypes of integrin family receptors are known, from which $\alpha_v\beta_3$, but also $\alpha_v\beta_5$ and $\alpha_v\beta_6$ are of well-studied subtypes recognizing the Arg-Gly-Asp (RGD) peptide (Figure 16), and their expression correlates with metastasis.

An enhanced $\alpha_v\beta_3$ expression is associated with angiogenesis, tumor growth, invasion, and metastasis. The $\alpha_v\beta_3$ integrins expression has been demonstrated in various endothelial and cancer cells such as breast, gastric, non-small cell lung, pancreatic, ovarian, and prostate cancer, oral squamous cell carcinoma, melanoma, or glioma [167]. Over the last decades, many radiolabeled bioactive molecules with the RGD motif have been synthesized and evaluated for the integrin $\alpha_v\beta_3$ -positive tumors targeting, providing useful conjugates for clinical translation (see summary in Table 11). Since 2018, a number of

traditional syntheses of novel BFCA-RGD conjugates has rapidly decreased due to the utilization of RGD peptides for a nanoparticle coupling.

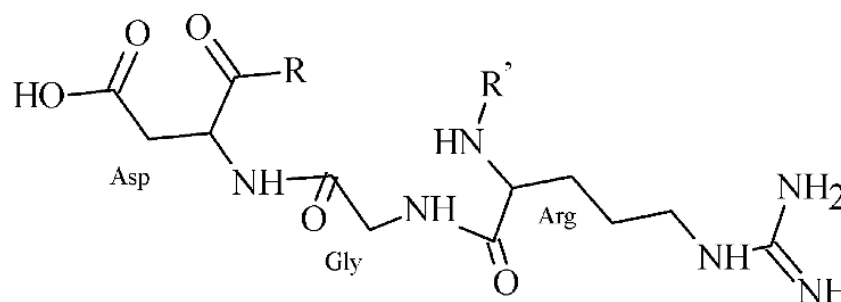


Figure 16. Structure of a peptide containing RGD sequence.

Table 11. Summary of radiolabeled RGD analogues for $\alpha_v\beta_3$ receptor-positive tumor imaging over past 3 years.

Composition of Studied Compounds	Results and Findings	Reference
- Metal Radionuclide	- Phase of Trials	
- BFCA	- Cancer Type Studied	
- Linker	- Imaging Technique Used	
- Peptide	- Benefits/Limitations/Conclusion	
- ⁶⁸ Ga - DOTA, TRAP, FSC, THP - glutamic acid - (RGD) ₃ , [c(RGDfK)] ₂	- preclinical in vitro, in vivo - renal, head and neck - microPET/CT - the highest tumor uptake for FSC- and THP-conjugates, but further studies on binding behavior to integrins needed	[168]
- ^{99m} Tc - glucoheptonate, D-penicillamine - Ahx - c(RGDfK)	- preclinical in vitro, in vivo - glioma - microSPECT/CT - [^{99m} Tc]Tc-[Pen-Ahx-c(RGDfK)] ₂ with the 10-fold higher integrin affinity than the monovalent (Pen-Ahx-c(RGDfK)), but high uptake in the liver, intestine, and kidney calls for an improvement of pharmacokinetics	[169]
- ^{99m} Tc - IDA - aspartic acid - [c(RGDfK)] ₂	- clinical, 6 patients - x - gamma camera - radiation doses of renal and biliary system comparable to other ^{99m} Tc-labeled peptides, further dosimetry studies needed for a risk-benefit assessment	[170]
- ⁶⁸ Ga - NOTA-NHS - 6-Ahx, cysteine - c(RGDyK), GE11	- preclinical in vitro, in vivo - lung - PET/CT - enhanced tumor accumulation of [⁶⁸ Ga]Ga-NOTA-RGD-GE11 than monomeric RGD-conjugate, but a modification of linkers needed for an improvement of pharmacokinetics	[171]
- ⁶⁸ Ga - NOTA - PEG3, symmetric β -glutamate linker - RGD2	- preclinical in vitro, in vivo - prostate - PET - significant limitations due to high renal and bladder accumulation, but low uptake in other organs	[172]

Table 11. Cont.

Composition of Studied Compounds - Metal Radionuclide - BFCA - Linker - Peptide	Results and Findings - Phase of Trials - Cancer Type Studied - Imaging Technique Used - Benefits/Limitations/Conclusion	Reference
- ^{99m}Tc - HYNIC, tricine, TPPTS - x - RGD2	- clinical, 20 patients - breast - gamma camera - good uptake in breast lesions and also metastatic sites in lymph nodes visible in 2 patients - useful easily available kit for further clinical studies	[173]
- ^{68}Ga - DOTA - glutamic acid - (cRGDFK)2	- preclinical in vitro, in vivo - lung - PET/CT - ^{68}Ga -labeled conjugate with highly hydrophilic properties, high tumor accumulation, moderate in vivo uptake in kidneys and intestine, with a potential for early detection of lung lesions	[174]

4.6. Other Radiometal Labeled Peptide Analogues for Imaging of Other Tumor Receptors

Neurotensin (NT), α -melanocyte stimulating hormone (α -MSH), substance P, and vasoactive intestinal peptide (VIP) represent other important radiometal labeled peptide analogues for imaging of various other significant tumor receptors (Figure 17).

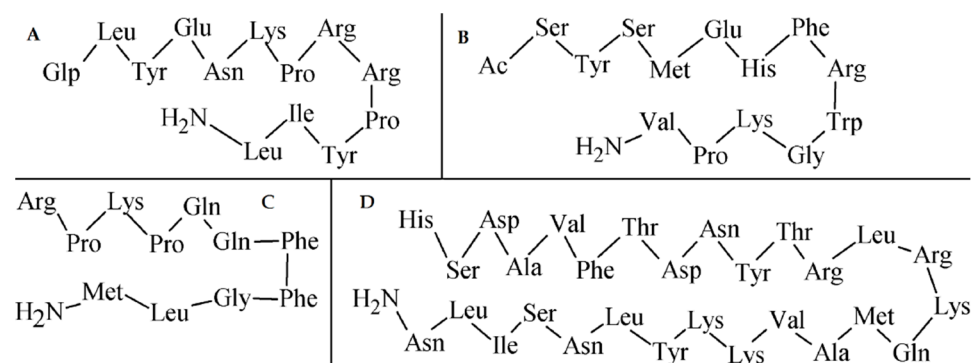


Figure 17. AA sequences of other important peptides for tumor imaging. (A) neurotensin; (B) α -MSH; (C) substance P; (D) VIP.

The NT is a neurotransmitter and hormone with a sequence of 13 AA, in which the C-terminal NT(8–13) is responsible for affinity and activity to a NT receptor. There are three types of the NT receptors: NTR₁–NTR₃, where NTR₁ is an extensively studied receptor and a promising target for cancer imaging. The NTR₁ overexpression has been demonstrated in a tumor progression, e.g., in pancreas and colon adenoma, but also in breast, lung, or prostate cancer, while the expression of NTR₂ has been reported in prostate cancer, lymphatic leukemia, and glioma [175]. Several NT analogues have been developed as effective targets for colorectal adenocarcinoma cells (Table 12).

The α -MSH is a neuropeptide with a sequence of 13 AA that is selectively bound to a melanocortine-1 receptor (MC1) overexpressed in leukocytes, melanocytes, and transformed melanoma cells, and is primarily responsible for a regulation of inflammatory state and skin pigmentation [176]. Numerous α -MSH analogues have been developed as attractive targets for melanoma radiodiagnosis or imaging (Table 12).

The substance P with a 11-AA sequence belongs to a family of tachykinins and exerts its activity through the G protein-coupled neurokinin receptors (NKR), i.e., NK₁R–NK₃R,

with the highest affinity of NK₁R. The substance P has been found in various cell systems bearing NK₁R, such as immune cells, monocytes, macrophages, lymphocytes, microglia, dendritic cells, bone marrow stem cells, and others. In the central nervous system, NK₁R are expressed in neurons, astrocytes, microglia, and cerebral endothelial cells [177]. Effects of the substance P in human organism include: immune and secretion stimulation, smooth muscle contraction (pulmonary, urinary, GIT, and vascular system), and is involved also in a pain transmission, vasodilatation, connective-tissue cell proliferation, and neuroimmune modulation [177]. Thus, substance P analogues and NK₁R antagonists have been synthesized and used for the NK₁R-positive tumor detection as shown in Table 12.

The VIP is a peptide with a 28 AA sequence that regulates various immune cells, promotes vasodilatation, growth and function of tumor cells. Its biological action is mediated through three classes of the G-protein-coupled receptors VPAC1, VPAC2, and PAC1. The receptors for VIP occurs in numerous tumor cells including thyroid, breast, lung, liver, pancreas, intestinal epithelial cells, colon, bladder, prostate, uterus, and neuroendocrine tumors [178,179].

Table 12. Summary of radiolabeled NT, α -MSH, substance P, and VIP analogues for other important receptor-positive tumor imaging over past 3 years.

Composition of Studied Compounds - Metal Radionuclide - BFCA - Linker - Peptide	Results and Findings - Phase of Trials - Cancer Type Studied - Imaging Technique Used - Benefits/Limitations/Conclusion	Reference
- ^{99m} Tc - HYNIC, EDDA, tricine - x - [Ac-Lys ⁵ , Pro ⁶ , β Ala ⁷ , Tle ¹²]NT(5–13)	- preclinical in vitro, in vivo - colorectal - gamma camera - useful for early tumor SPECT staging due to appropriate tumor accumulation, high stability, low liver accumulation, and high kidney excretion	[180]
- ⁶⁸ Ga - DOTA(tBu) ₃ - 4- amino piperidin-1-yl-acetic acid - Lys ⁸ -Lys ⁹ -Pro ¹⁰ -Tyr ¹¹ -Ile ¹² -Leu ¹³ -OH modified with TMSAla ^{12/13}	- preclinical in vitro, in vivo - colorectal - microPET/CT - good NTR1 selectivity and prolonged plasmatic half-life of [⁶⁸ Ga]Ga-(TMSAla ¹³)-conjugate; further in vivo uptake and impact of other metals (¹¹¹ In, ¹⁷⁷ Lu, ¹⁶¹ Tb) under investigation	[181]
- ^{99m} Tc - DPA - Ahx- β Ala, ethylene glycol (EG) based linker - Nle-Asp-His-D-Phe-Arg-Trp-Gly-NH ₂	- preclinical in vitro, initial in vivo - melanoma - x - high in vitro stability of [^{99m} Tc]Tc-tricarbonyl-DPA base; EG linker more useful than Ahx	[182]
- ¹¹¹ In - NHS-DOTA (3-arm), SCN-Bn-DOTA (4-arm) - x - α -MSH	- preclinical in vitro, in vivo - melanoma - SPECT - higher lipophilicity, higher MC1-R affinity, and relatively higher stability of 4-arm DOTA-conjugates than 3-arm	[183]
- ⁶⁴ Cu - SCN-NOTA, bispidine carbonate, SCN-dipyridylmethyl-TACN - Ahx- β -Ala - Nle-Asp-His-D-Phe-Arg-Trp-Gly-NH ₂	- preclinical in vitro, initial in vivo - melanoma - gamma counter - high hydrophilicity and sufficient MC1R-affinity of ⁶⁴ Cu-conjugate, but lower than that of [¹²⁵ I]I-NDP-MSH	[184]
- ^{99m} Tc - NOTA, NODAGA - Gly-Gly-Nle - c[Asp-His-DPhe-Arg-Trp-Lys]-NH ₂	- preclinical in vitro, in vivo - melanoma - nanoSPECT/CT - NOTA-conjugate with better tumor targeting and biodistribution properties; study with rhenium-188 suggested	[185]

Table 12. Cont.

Composition of Studied Compounds - Metal Radionuclide - BFCA - Linker - Peptide	Results and Findings - Phase of Trials - Cancer Type Studied - Imaging Technique Used - Benefits/Limitations/Conclusion	Reference
- ^{99m}Tc , ^{177}Lu - tris(2-mercaptoethyl)-amine, isocyanobutyric acid succinimidyl ester, DOTA - x - various SP analogues	- preclinical in vitro - glioblastoma - x - lipophilic conjugates with specific tumor binding, high stability in buffer solutions, but lower stability in human serum	[186]
- ^{64}Cu , ^{67}Ga - NOTA - x - NK ₁ R antagonist	- preclinical in vitro, in vivo - kidney - PET/CT - high in vivo stability, tumor uptake and good liver and renal clearance of [^{64}Cu]Cu-NOTA-conjugate	[187]
- ^{68}Ga - NODAGA - PEG _x - BBN(7-14), PACAP-27	- preclinical in vitro - x - improved stability of heterobivalent conjugates and comparable uptakes in tumor cells to those of monomers, further evaluation for in vivo PET/CT in progress	[188]
- ^{68}Ga - NODAGA, DOTA - x - PACAP-27	- preclinical in vitro, in vivo - breast - PET/CT - low in vivo stability, but greater VPAC-affinity and tumor delineation only for NODAGA-conjugate	[189]
- ^{64}Cu - N ₂ S ₂ chelator - x - TP3805	- preclinical in vitro, in vivo - brain - microPET/CT - more specific brain tumor delineation than [^{18}F]FDG, further investigation for clinical translation warranted	[190]

4.7. Small Peptide Inhibitors of Proteins for Protein-Positive Tumor Imaging

Many protein interactions in a biological system are responsible for an origination or progression of various diseases including cancer. In recent years, inhibitors of such proteins based on small peptide biomolecules are widely developed and investigated. This subsection covers the latest radiolabeled peptide inhibitors of the prostate-specific membrane antigen (PSMA) and fibroblast activation protein (FAP) for imaging of related tumors (see summarized studies in Table 13).

The PSMA is a membrane-bound folate gamma glutamyl-carboxypeptidase II, which is physiologically present in various tissues, e.g., salivary glands, ovary, prostate epithelium, and astrocytes [191]. From the cancerous cells, it is primarily expressed in benign and malignant prostatic tissue [192]. However, studies on the PSMA-expression in also other tumor types are available, including breast, gastric, and colorectal cancer, lung and renal carcinoma, and brain tumors [193–198]. Thus, PSMA has become one of the most promising and extensively evaluated molecular targets in nuclear medicine. Research was mainly focused on monoclonal antibodies, but various radiolabeled small peptide-based inhibitors containing Glu-C(O)-Lys (EuK) sequence (see Figure 18A) have been recently developed to effectively localize and treat related tumors. Other two functionalities, i.e., phosphonates and thiols, with affinity to PSMA have been identified. The most widely used example of such inhibitor is the [^{68}Ga]Ga-PSMA-11 (i.e., ^{68}Ga -labeled Glu-NH-CO-NH-Lys(Ahx)-HBED-CC) [199]. At present, it is included in many clinical trials that monitor various conditions in a prostate cancer management.

Another extensively studied protein with selective expression in several tumor types is FAP, a serine protease. The FAP protein has been associated with fibrosis, inflammation and cancer, and is undetectable in a majority of normal adult tissues [200]. Several works revealed its localization not only in activated fibroblasts [201], but also in endothelial cells and macrophages [202,203]. The participation of FAP in a cell invasiveness, proliferation, migration and tumor vascularization has been described [204]. The FAP overexpression and activation has been observed in various malignancies, e.g., pancreatic, hepatocellular, lung, breast, colorectal, or ovarian [205–210]. Different strategies are investigated to target FAP activity such as (i) probes with fluorescent moiety, (ii) prodrug delivery systems, (iii) FAP inhibitors (FAPI), and (iv) immune-based pathways [211]. Radiolabeled peptide FAPI based on 2-cyanopyrrolidin-quinoline carboxamide structure (Figure 18B) were developed [212] and then FAPI linkers have been modified to improve pharmacokinetic properties, tumor binding, and PET images [213]. Further structural modifications and clinical studies are underway and thus FAPI represent new attractive imaging and therapeutic options for oncological diseases.

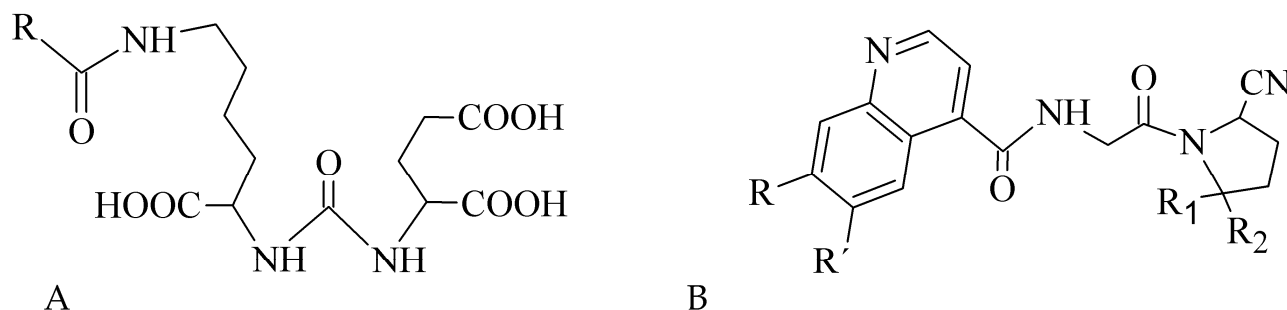


Figure 18. Structural motifs of small peptide inhibitors of proteins. (A) EuK motif as a base for PSMA inhibitors, (B) 2-cyanopyrrolidin-quinoline carboxamides as a base for FAP inhibitors.

Table 13. Summary of radiolabeled small peptide inhibitors for PSMA- and FAP-positive tumor imaging over past 3 years.

Composition of Studied Compounds	Results and Findings	Reference
- Metal Radionuclide	- Phase of Trials	
- BFCA	- Cancer Type Studied	
- Linker	- Imaging Technique Used	
- Peptide	- Benefits/Limitations/Conclusion	
- ^{68}Ga - THP - Ahx - EuK motif (PSMA)	- clinical, 118 patients - prostate - PET/CT - PET/CT impacts on management decisions in high-risk prostate cancer prior to radical therapy and biochemical recurrence	[214]
- $^{99\text{m}}\text{Tc}$ - HYNIC - Gly-Ala-Asp-NaphthylAla - PSMA	- preclinical in vitro, in vivo - prostate - SPECT/CT - [$^{99\text{m}}\text{Tc}$]Tc-HYNIC-conjugate with approximately similar pharmacokinetic and binding properties to [^{68}Ga]Ga-PSMA-11, and great SPECT/CT visualization of tumor	[215]
- ^{64}Cu - cyclam derivatives - naphthylAla, cyclohexane-carboxylic acid - PSMA	- preclinical in vitro, in vivo; first patient - prostate - PET - [^{64}Cu]Cu-CA003 applied to first patient due to the best pharmacokinetic and imaging properties	[216]

Table 13. Cont.

Composition of Studied Compounds - Metal Radionuclide - BFCA - Linker - Peptide	Results and Findings - Phase of Trials - Cancer Type Studied - Imaging Technique Used - Benefits/Limitations/Conclusion	Reference
- ^{68}Ga - HBED-CC - Ahx - PSMA	- clinical - glioblastoma multiforme (GBM) - PET/CT - [^{68}Ga]Ga-PSMA-11 as a highly promising agent for diagnosis of recurrent disease in patients with GBM due to low tumor-to-liver ratio and increased accumulation in recurrent lesions	[217]
- ^{64}Cu , ^{67}Cu - MeCoSar derivative - iodophenyl-1,2,3-triazolyl derivative - PSMA	- preclinical in vitro, in vivo - prostate - microPET/CT - Cu-labeled agents as promising alternatives to ^{68}Ga -/ ^{177}Lu -analogues in centers with limited access to these ligands	[77]
- ^{68}Ga , ^{89}Zr - DFO squaramide - p-aminomethylbenzoic acid - PSMA	- preclinical in vitro, in vivo - prostate - PET/CT - improved tumor uptake of bivalent inhibitors with 2 EuK motifs, ^{89}Zr -complex as a promising alternative to ^{68}Ga -analogue	[89]
- ^{44}Sc - AAZTA derivatives - naphthylAla - PSMA	- preclinical in vitro, in vivo - prostate - PET/MRI - dynamic PET images showed high tumor uptake, rapid clearance from investigated tissue, very low accumulation at 150 min post-injection in the abdominal organs, lung, heart and brain, but higher in bladder	[218]
- ^{68}Ga , ^{177}Lu - DOTA - piperazine - FAPI-02,-04	- clinical, 23 patients together - fibrosarcoma, pancreatic, breast, lung, colon, thyroid, head and neck - microPET, PET/CT - [^{68}Ga]Ga-FAPI-02 with TBR equal to or even better than [^{18}F]FDG, PET/CT with ^{68}Ga -probes can be performed without fasting and resting time	[219–221]
- ^{68}Ga - DOTA - piperazine - FAPI-04	- clinical, 80 patients - 28 different tumor entities - PET/CT - the highest uptake in breast, esophagus, lung, pancreatic, head-neck, and colorectal cancer; FAPI limitations similar to those of FDG for renal and thyroid cancer	[222]
- ^{68}Ga - DOTA - piperazine - FAPI-02/-04	- preclinical in vitro, in vivo; clinical, 18 patients - glioma - microPET, PET/CT - IDH-wildtype glioblastomas and grade III/IV, but not grade II IDH-mutant gliomas showed elevated tracer uptake	[223]
- ^{64}Cu - DOTA - piperazine - FAPI-04	- preclinical in vitro, in vivo - pancreatic - microPET/CT - in vivo accumulation in tumor or normal organs significantly higher for [^{64}Cu]Cu-FAPI-04 than [^{68}Ga]Ga-FAPI-04, except in the heart	[224]

Table 13. Cont.

Composition of Studied Compounds - Metal Radionuclide - BFCA - Linker - Peptide	Results and Findings - Phase of Trials - Cancer Type Studied - Imaging Technique Used - Benefits/Limitations/Conclusion	Reference
- ⁶⁸ Ga - DOTA - piperazine - FAPI-04	- clinical, 17 patients - hepatic - PET/CT - high sensitivity in poorly differentiated hepatic tumors	[225]
- ⁶⁸ Ga - DOTA - diazabicyclo[2.2.1]heptan containing linker - FAPI-46	- clinical, 6 patients - different tumor types - PET/CT - high TBR increasing over time and favorable dosimetry profile (highest effective doses were in bladder wall, ovaries, red marrow)	[226]
- ⁶⁸ Ga - DOTA - piperazine - FAPI-02/-04	- clinical, 13 patients - glioblastoma - PET/MRI - MRI- and FAP-specific gross tumor volumes were not congruent	[227]
- ⁶⁸ Ga - DOTA - piperazine - FAPI-04	- clinical, 68/75 patients - different tumor types - PET/CT - higher TBR of FAPI compared to FDG for brain metastases, FAPI identified more lesions for hepatic and peritoneal tumor manifestations, and had higher sensitivity in a detection of lymphonodal, osseous and visceral metastases	[228,229]
- ^{99m} Tc - <i>o</i> tBu-imidazol containing BFCA - piperazine - FAPI-19/-34	- preclinical in vitro, in vivo; clinical, 2 patients - pancreatic, ovarian - SPECT - [^{99m} Tc]Tc-FAPI-34 accumulation in tumor lesions similar to [⁶⁸ Ga]Ga-FAPI-46	[230]

4.8. Radiometal Labeled Sulfonamide-Based Analogues for Tumor Hypoxia Imaging

Hypoxia, a phenomenon when a level of oxygen is below its demands, is a common feature for tumor development and progression. Many solid tumors have regions permanently or transiently exposed to hypoxia because of aberrant vascularization and a poor blood supply [231]. Since hypoxia is a key component in cellular expression, tumor blood vessel formation, cancer progression, metastasis, often leading to cell death, a current research in this area is focused to an early detection and selective monitoring or suppression of hypoxic tissues to effectively minimize all possible complications associated with this phenomenon. Many studies have been comprised of radiolabeled small nitroimidazole derivatives [232–235], and monoclonal antibodies [236,237], resulting in a development of new agents capable of accessing to overexpressed proteins under hypoxic state (i.e., hypoxia inducible factor HIF-1 regulated genes for carbonic anhydrase CA IX, vascular endothelial growth factor, angiopoietin-2, etc. [238]). Nevertheless, small sulfonamide- and peptide-based biomolecules labeled with metal radionuclides have been studied for imaging of various hypoxic tumor cells overexpressing CA IX as one of the prominent gene in the HIF-induced processes (see summary in Table 14). A highly specific binding of various sulfonamide derivatives with amino-acid substituents has been demonstrated in our several recent works. For example, an illustrative superposition and intermolecular interaction diagram of potential 1,3,5-triazinyl-sulfonamide inhibitor docked into the active site of human CA IX are in Figure 19A,B.

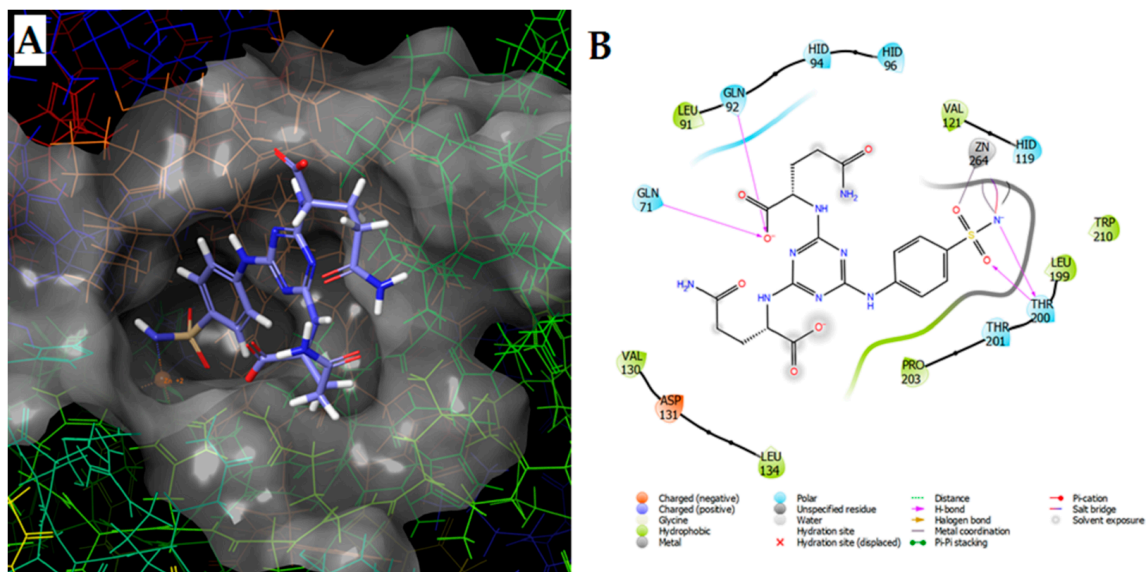


Figure 19. Position of sulfonamide-derived hCA IX inhibitor docked into the active site of hCA IX (A) and its intermolecular interaction diagram (B) [239].

Table 14. Summary of radiolabeled small ligands for CA IX-positive tumor hypoxia imaging over past 3 years.

Composition of Studied Compounds - Metal Radionuclide - BFCA - Linker - Biomolecule	Results and Findings - Phase of Trials - Cancer Type Studied - Imaging Technique Used - Benefits/Limitations/Conclusion	Reference
- ^{111}In - DOTA-ester - x - bis-ureidosulfonamide derivative	- preclinical in vitro, in vivo - breast, colorectal - SPECT/CT - rapid clearance from blood and muscle, and selective accumulation within CAIX expressing colon cancer cells	[240]
- $^{99\text{m}}\text{Tc}$ - dipyridylamine, IDA - x - sulfonamide, sulfocoumarin	- preclinical in vitro, initial in vivo - colorectal - x - significant limitations in very low tumor uptake and much higher liver uptake	[241]
- ^{68}Ga - CBT, NODA, pyridine, DOTA-NHS, NODAGA-NHS - Asp-Arg-Asp, PEG ₂ linker - acetazolamide	- synthesis, initial in vitro - x - useful CBT/1,2-aminothiols click reaction for CAIX ligands with in vitro stability developed	[113]
- $^{99\text{m}}\text{Tc}$ - hydroxamamide (Ham), methyl-substituted-Ham (MHam) - x - sulfonamide, ureidosulfonamide	- synthesis, initial in vitro, in vivo - renal and colorectal - gamma counter - [$^{99\text{m}}\text{Tc}$]Tc-MHam-bivalent conjugate with the highest tumor specificity useful for further studies	[242]
- ^{111}In - DOTA-bis(tBu)ester - x - imidazothiadiazole sulfonamide	- preclinical in vitro, in vivo - breast and colorectal - SPECT/CT - favorable in vivo properties of [^{111}In]In-DO3A-IS1 with selective binding and accumulation in CAIX-expressing colon cancer	[243]

5. Concluding Remarks and Future Perspectives

Various chemical types of metallic radiopharmaceuticals for use in oncology are approved by the European Medicines Agency or U.S. Food and Drug Administration. Apart from these registered radioactive medicines, a much larger scale of radiolabeled bioactive ligands is under investigation in nuclear research or clinical trials. In this review, recent advances in the radiolabeling process of amino-acid based biomolecules, the most commonly used metal radionuclides, their chemistry and BFCA, as well as the most important peptide receptor families (including currently the most perspective field of PSMA and FAP ligands), were critically discussed. Continual efforts in proposing new structures with improved pharmacokinetic properties for selective targeting of cancer cells and effective utilization in imaging techniques should be guaranteed. The disease imaging on a molecular level, as well as radionuclide availability on-site, lower radiation burden, detection of early stage problem, and monitoring of a response to treatment in the combination with targeted therapy for a personalized approach to a patient, have a great potential to bring additional valuable outputs in the field of nuclear medicine in future.

Over the past years, great progress in a radiolabeling with metallic radionuclides has been demonstrated, owing to a development of many new chelators (or new derivatives of well-known traditional chelators) and linkers for an effective connection between metals and biomolecules. Modern chelators such as TRAP, THP, and FSC for gallium-68, DFO for zirconium-89, sarcophagines for copper-64, tricarbonyl and [N,S,X]-type chelators for technetium-99m and their modifications have been designed to improve binding affinity and pharmacokinetic properties of a radiolabeled probe for its molecular target. In spite of remarkable progress, there is still an enormous need to develop target specific compounds with improved pharmacokinetics and selectivity to a desired in vivo target, because many studies have confirmed various complications in the development. These are mainly lower stability, higher toxicity, adverse pharmacokinetic behavior, and higher retention of radioactivity in studied material in vivo and in vitro. In this context, amino acid moieties proved to be ones of the most suitable linkers to complete a target-specific structure. Optimized structures of some of the newly developed radiolabeled biomolecules should provide enhanced affinity and selectivity to the onco-receptors, lower radiation dosage for patient, decreased interactions with other drugs or physiological proteins, without misrepresenting results, and, by that, a more favorable utilization in diagnostic nuclear medicine over other imaging techniques (e.g., MRI, CT).

Peptides, as amino acid based biomolecules, represent current and future important tools in a development of target-specific radiolabeled compounds. It is due to a high degree of their compatibility with many protein structures overexpressed in various diseases, including cancer, as the second leading cause of death globally. Current research, with a promising perspective, is directed mainly towards peptide radiolabeled agents that are aimed at proteins overexpressed in pancreatic, colorectal, prostate, and brain tumors. These types belong to the most frequently diagnosed and the most severe cancers. The integrin $\alpha_v\beta_3$ receptors from traditional receptor families and PSMA, as well as FAP ligands are very attractive and perspective probes due to their intense association and overexpression within a variety of cancer cells and new vasculature in general, and so tumor growth, proliferation, and metastasis.

As emerged from the reviewed studies dealing with an implementation of imaging methods (PET, SPECT, etc.), in nuclear medicine research, gallium-68, DOTA-based chelators, and amino acid linkers are currently dominating in the research of new potential diagnostic and imaging agents. In centers, where ^{68}Ga -compounds cannot be used due to gallium unavailability, alternative PET labels were introduced. For example, yttrium-86 or zirconium-89 could be employed since a remarkable development in small medical cyclotrons has been achieved over past years. However, there are still new $^{99\text{m}}\text{Tc}$ -labeled analogues for SPECT imaging as an alternative method of PET tracers. Other interesting non-standard radionuclides such as cobalt-55, scandium-44, titanium-45, and manganese-52 are increasingly utilized in preclinical studies and could be a merit of future investi-

gations in clinical field. These non-standard metal radionuclides with their therapeutic pairs represent the highly attractive labels for development of theranostic approaches as precise predictive biomarkers of a response to therapy strategies. The inherent part of a diagnostic or imaging process is an applied imaging technique. It is evident that hybrid methods of SPECT and PET combined with CT is of routine. The ongoing studies could be focused on a development of probes and methodologies with high anatomical and functional sensitivity, spatial resolution, as well as mentioned superior pharmacokinetic profile for a better disease management using SPECT and PET with MRI as an important tool to improve the diagnostics, staging and planning of treatment strategy.

Author Contributions: M.B.M. conceptualization, writing of review, editing; P.M. conceptualization, editing, corrections, and supervision. All authors have read and agreed to the published version of the manuscript.

Funding: This work was supported by the projects APVV-15-0585, VEGA 1/0463/18, KEGA 027UK-4/2020, and the Grant of Faculty of Pharmacy, Comenius University in Bratislava No. FaF/32/2020.

Institutional Review Board Statement: Not applicable.

Informed Consent Statement: Not applicable.

Data Availability Statement: No new data were created or analyzed in this study. Data sharing is not applicable to this article.

Acknowledgments: Some experimental results presented in this work were obtained in the Toxicological and Antidoping Center at the Faculty of Pharmacy, Comenius University in Bratislava.

Conflicts of Interest: The authors declare no conflict of interest.

Abbreviations

AA	amino acid
AAZTA	6-amino-6-methylperhydro-1,4-diazepinetetraacetic acid
AHDA	amino-hexanedioic-1-acid
AHX	6-aminohexanoic acid
APCA	2-aminoethyl-piperazine-1-carboxylic acid
BBN	bombesin
BFCA	bifunctional chelating agent
hCA	human carbonic anhydrase
CBT	2-cyanobenzothiazole
CCK(R)	cholecystokinin (receptor)
c(RGDfK)	cyclo(-Arg-Gly-Asp-D-Phe-Lys)
CT	computed tomography
CuAAC	Cu(I)-catalyzed azide-alkyne cycloaddition
DATA	6-amino-1,4-diazepine-triacetate
DOTA	2,2',2'',2'''-(1,4,7,10-tetraazacyclododecane-1,4,7,10-tetrayl)tetraacetic acid
DOTANOC	DOTA-Nal ³ -octreotide
DOTATATE	DOTA-Tyr ³ -octreotate
DOTATOC	DOTA-Tyr ³ -octreotide
DPA	5-(bis(pyridin-2-yl)methyl)amino)pentanoic acid
DTPA	diethylenetriamine pentaacetic acid
EDDA	ethylenediamine diacetic acid
EDTA	ethylenediamine tetraacetic acid
FAP	fibroblast activation protein
GE11	Tyr-His-Trp-Tyr-Gly-Tyr-Thr-Pro-Gln-Asn-Val-Ile
GEP NET	gastroenteropancreatic neuroendocrine tumors
GLP	glucagon-like peptide
GRPR	gastrin-releasing peptide receptor
HBED-CC	<i>N,N'</i> -bis-[2-hydroxy-5-(carboxyethyl)benzyl]ethylenediamine- <i>N,N'</i> -diacetic acid
HIF	hypoxia inducible factor

HPLC-DAD	high performance liquid chromatography-diode array detection
HYNIC	6-hydrazinopyridin-3-carboxylic acid
IDA	iminodiacetic acid
IEDDA	inverse electron-demand Diels-Alder reaction
JR11	p-Cl-Phe-cyclo(D-Cys-Aph(Hor)-D-Aph(cbm)-Lys-Thr-Cys)D-Tyr-NH ₂
MAG3	mercaptoacetylglycylglycylglycine
MC	melanocortin (receptor)
MG11	[3-MP ⁰ -D-Glu ¹ ,desGlu ²⁻⁶]-Ala-Tyr-Gly-Trp-Met-Asp-Phe-NH ₂
MRI	magnetic resonance imaging
NeoBOMB1	D-Phe-Gln-Trp-Ala-Val-Gly-His-NH-CH[CH ₂ -CH(CH ₃) ₂] ₂
NET	neuroendocrine tumors
NHS	N-hydroxysuccinimidyl-ester
NKR	neurokinin receptor
NODAGA	1,4,7-triazacyclononane-1-glutaric acid-4,7-diacetic acid
NODAPA	1,4,7-triazacyclononane-1,4-diacetic acid-7-p-phenylacetic acid
NODASA	1,4,7-triazacyclononane-1-succinic acid-4,7-diacetic acid
NOTA	2,2',2''-(1,4,7-triazanonane-1,4,7-triyl)triacetic acid
NOTP	1,4,7-Triazacyclononane-1,4,7-tri(methylene phosphonic acid)
NP	nanoparticle
NSCLC	non-small cell lung cancer
NT(R)	neurotensin receptor
PA1	cyclo[HyPro-Phe-d-Trp-Lys-Tyr(Bzl)-Phe]
PAC-1	procaspase-activating compound receptor
PACAP	pituitary adenylate cyclase-activating peptide
PCTA	3,6,9,15-tetraazabicyclo[9.3.1]pentadeca-1(15),11,13-triene-3,6,9-triacetic acid
PEG	polyethylene glycol
PET	positron emission tomography
PC	prostate cancer
PSMA	prostate-specific membrane antigen
RGD	arginine-glycine-aspartic acid
RM26	1,4,7-triazacyclononane-N,N,N-triacetic acid-D-Phe-Gln-Trp-Ala-Val-Gly-His-Sta-Leu-NH ₂
RM2	DOTA-4-amino-1-carboxymethylpiperidine-D-Phe-Gln-Trp-Ala-Val-Gly-His-Sta-Leu-NH ₂
SERRS	surface-enhanced resonance Raman scattering
SPAAC	strain-promoted azide-alkyne cycloaddition
SPECT	single-photon emission computed tomography
SPPS	solid phase peptide synthesis
SST(R)	somatostatin (receptor)
TBR	tumor-to-background ratio
TETA	2,2',2'',2'''-(1,4,8,11-tetraazacyclotetradecane-1,4,8,11-tetrayl)tetraacetic acid
THP	tris(hydroxypyridinone)
TMSAla	(L)-trimethylsilylalanine
TOC	Tyr ³ -octreotide
TPPTS	trisodium triphenylphosphine-3,3',3''-trisulfonate
TRAP	1,4,7-triazacyclononane-1,4,7-tris(methylene(2-carboxyethylphosphinic acid))
UV	ultraviolet (detection)
VIP	vasoactive intestinal peptide
VPAC	receptor for vasoactive intestinal peptide
α-MSH	α-melanocyte stimulating hormone

References

- Okarvi, S. Peptide-based radiopharmaceuticals and cytotoxic conjugates. *Cancer Treat. Rev.* **2008**, *34*, 13–26. [[CrossRef](#)]
- Fani, M.; Mäcke, H.R. Radiopharmaceutical development of radiolabelled peptides. *Eur. J. Nucl. Med. Mol. Imaging* **2012**, *39*, 11–30. [[CrossRef](#)] [[PubMed](#)]
- Liu, S. Bifunctional coupling agents for radiolabeling of biomolecules and target-specific delivery of metallic radionuclides. *Adv. Drug Deliv. Rev.* **2008**, *60*, 1347–1370. [[CrossRef](#)]

4. Boschi, A.; Uccelli, L.; Martini, P. A picture of modern Tc-99m radiopharmaceuticals: Production, chemistry, and applications in molecular imaging. *Appl. Sci.* **2019**, *9*, 2526. [[CrossRef](#)]
5. Follacchio, G.A.; De Feo, M.S.; De Vincentis, G.; Monteleone, F.; Liberatore, M. Radiopharmaceuticals Labelled with Copper Radionuclides: Clinical Results in Human Beings. *Curr. Radiopharm.* **2018**, *11*, 22–33. [[CrossRef](#)] [[PubMed](#)]
6. Papagiannopoulou, D. Technetium-99m radiochemistry for pharmaceutical applications. *J. Label. Compd. Radiopharm.* **2017**, *60*, 502–520. [[CrossRef](#)]
7. MacPherson, D.S.; Fung, K.; Cook, B.E.; Francesconi, L.C.; Zeglis, B.M. A brief overview of metal complexes as nuclear imaging agents. *Dalton Trans.* **2019**, *48*, 14547–14565. [[CrossRef](#)] [[PubMed](#)]
8. Meyer, J.P.; Adumeau, P.; Lewis, J.S.; Zeglis, B.M. Click Chemistry and Radiochemistry: The First 10 Years. *Bioconj. Chem.* **2016**, *27*, 2791–2807. [[CrossRef](#)] [[PubMed](#)]
9. Burke, B.P.; Clemente, G.S.; Archibald, S.J. Recent advances in chelator design and labelling methodology for ⁶⁸Ga radiopharmaceuticals. *J. Label. Compd. Radiopharm.* **2014**, *57*, 239–243. [[CrossRef](#)] [[PubMed](#)]
10. Bolzati, C.; Carta, D.; Salvarese, N.; Refosco, F. Chelating systems for ^{99m}Tc/ ¹⁸⁸Re in the development of radiolabeled peptide pharmaceuticals. *AntiCancer Agents Med. Chem.* **2012**, *12*, 428–461. [[CrossRef](#)]
11. Tolmachev, V.; Stone-Elander, S. Radiolabelled proteins for positron emission tomography: Pros and cons of labelling methods. *Biochim. Biophys. Acta* **2010**, *1800*, 487–510. [[CrossRef](#)]
12. Brechbiel, M.W. Bifunctional Chelates for Metal Nuclides. *Q. J. Nucl. Med. Mol. Imaging* **2008**, *52*, 166–173. [[PubMed](#)]
13. Zhou, Y.; Li, J.; Xu, X.; Zhao, M.; Zhang, B.; Deng, S.; Wu, Y. ⁶⁴Cu-based Radiopharmaceuticals in Molecular Imaging. *Technol. Cancer Res. Treat.* **2019**, *18*. [[CrossRef](#)] [[PubMed](#)]
14. Reubi, J.C. Peptide receptors as molecular targets for cancer diagnosis and therapy. *Endocr. Rev.* **2003**, *24*, 389–427. [[CrossRef](#)]
15. Rezazadeh, F.; Sadeghzadeh, N. Tumor targeting with ^{99m}Tc radiolabeled peptides: Clinical application and recent development. *Chem. Biol. Drug Des.* **2018**, *93*, 205–221. [[CrossRef](#)] [[PubMed](#)]
16. Tornesello, A.L.; Tornesello, M.L.; Buonaguro, F.M. An Overview of Bioactive Peptides for in vivo Imaging and Therapy in Human Diseases. *Mini Rev. Med. Chem.* **2017**, *17*, 758–770. [[CrossRef](#)] [[PubMed](#)]
17. Bartholoma, M. Recent Developments in the Design of Bifunctional Chelators for Metal-based Radiopharmaceuticals Used in Positron Emission Tomography. *Inorg. Chim. Acta* **2012**, *389*, 36–51. [[CrossRef](#)]
18. Wängler, B.; Schirmacher, R.; Bartenstein, P.; Wängler, C. Chelating Agents and their Use in Radiopharmaceutical Sciences. *Mini Rev. Med. Chem.* **2011**, *11*, 968–983. [[CrossRef](#)]
19. Tsiou, M.I.; Knapp, C.E.; Foley, C.A.; Ma, M.T. Comparison of macrocyclic and acyclic chelators for gallium-68 radiolabelling. *RSC Adv.* **2017**, *7*, 49586–49599. [[CrossRef](#)]
20. Jamous, M.; Haberkorn, U.; Mier, W. DOTA-tris(OPp ester) as a bifunctional prochelator for the preparation of DOTA-peptide conjugates. *Tetrahedron Lett.* **2012**, *53*, 6810–6814. [[CrossRef](#)]
21. Kilian, K. ⁶⁸Ga-DOTA and analogues: Current status and future perspectives. *Rep. Pract. Oncol. Radiother.* **2014**, *19*, S13–S21. [[CrossRef](#)]
22. Abrams, M.J.; Juweid, M.; Strauss, H.W.; Fischman, A.J. Technetium-99m-human polyclonal IgG radiolabeled via the hydrazino nicotinamide derivative for imaging focal sites of infection in rats. *J. Nucl. Med.* **1990**, *31*, 2022–2028. [[PubMed](#)]
23. Dearling, J.L.J.; Blower, P.J. Redox-active metal complexes for imaging hypoxic tissues: Structure-activity relationships in copper(II) bis(thiosemicarbazone) complexes. *Chem. Commun.* **1998**, *22*, 2531–2532. [[CrossRef](#)]
24. Blower, P.J.; Castle, T.C.; Cowley, A.R.; Went, M.J. Structural trends in copper(II) bis(thiosemicarbazone) radiopharmaceuticals. *Dalton Trans.* **2003**, *23*, 4416–4425. [[CrossRef](#)]
25. Boswell, C.A.; Regino, C.A.S.; Baidoo, K.E.; Brechbiel, M.W. Synthesis of a cross-bridged cyclam derivative for peptide conjugation and ⁶⁴Cu radiolabeling. *Bioconj. Chem.* **2008**, *19*, 1476–1484. [[CrossRef](#)] [[PubMed](#)]
26. Sun, X.; Wuest, M.; Weisman, G.R.; Anderson, C.J. Radiolabeling and in vivo behavior of copper-64-labeled cross-bridged cyclam ligands. *J. Med. Chem.* **2002**, *45*, 469–477. [[CrossRef](#)]
27. Tan, K.V.; Pellegrini, P.A.; Skelton, B.W.; Barnard, P.J. Triamidetriamine bearing macrobicyclic and macrotricyclic ligands: Potential applications in the development of copper-64 radiopharmaceuticals. *Inorg. Chem.* **2014**, *53*, 468–477. [[CrossRef](#)] [[PubMed](#)]
28. Cai, H.; Fissekis, J.; Conti, P.S. Synthesis of a novel bifunctional chelator AmBaSar based on sarcophagine for peptide conjugation and ⁶⁴Cu radiolabelling. *Dalton Trans.* **2009**, 5395–5400. [[CrossRef](#)]
29. Langen, K.J.; Broer, S. Molecular Transport Mechanisms of Radiolabeled Amino Acids for PET and SPECT. *J. Nucl. Med.* **2004**, *45*, 1435–1436.
30. Huang, C.; McConathy, J. Radiolabeled Amino Acids for Oncologic Imaging. *J. Nucl. Med.* **2013**, *54*, 1007–1010. [[CrossRef](#)] [[PubMed](#)]
31. Merrifield, R.B. Solid phase peptide synthesis. I. The synthesis of a tetrapeptide. *J. Am. Chem. Soc.* **1963**, *85*, 2149–2154. [[CrossRef](#)]
32. Amblard, M.; Fehrentz, J.A.; Martinez, J.; Subra, G. Methods and protocols of modern solid phase peptide synthesis. *Mol. Biotechnol.* **2006**, *33*, 239–254. [[CrossRef](#)]
33. Čerovský, V.; Bordusa, F. Protease-catalyzed fragment condensation via substrate mimetic strategy: A useful combination of solid-phase peptide synthesis with enzymatic methods. *J. Pept. Res.* **2000**, *55*, 325–329. [[CrossRef](#)] [[PubMed](#)]
34. Neimark, J.; Briand, J.P. Development of a fully automated multichannel peptide synthesizer with integrated TFA cleavage capability. *Pept. Res.* **1993**, *6*, 219–228.

35. Evans, B.J.; King, A.T.; Katsifis, A.; Matesic, L.; Jamie, J.F. Methods to Enhance the Metabolic Stability of Peptide-Based PET Radiopharmaceuticals. *Molecules* **2020**, *25*, 2314. [[CrossRef](#)]
36. Morais, G.R.; Paulo, A.; Santos, I. Organometallic complexes for SPECT imaging and/or radionuclide therapy. *Organometallics* **2012**, *31*, 5693–5714. [[CrossRef](#)]
37. Hahn, E.M.; Casini, A.; Kuehn, F.E. Re(VII) and Tc(VII) trioxo complexes stabilized by tridentate ligands and their potential use as radiopharmaceuticals. *Coord. Chem. Rev.* **2014**, *276*, 97–111. [[CrossRef](#)]
38. Zhao, Z.Q.; Yang, Y.; Fang, W.; Liu, S. Comparison of biological properties of ^{99m}Tc -labeled cyclic RGD Peptide trimer and dimer useful as SPECT radiotracers for tumor imaging. *Nucl. Med. Biol.* **2016**, *43*, 661–669. [[CrossRef](#)]
39. Ortiz-Arzate, Z.; Santos-Cuevas, C.L.; Izquierdo-Sánchez, V. Kit preparation and biokinetics in women of ^{99m}Tc -EDDA/HYNIC-E-[c(RGDfK)]₂ for breast cancer imaging. *Nucl. Med. Commun.* **2014**, *35*, 423–432. [[CrossRef](#)] [[PubMed](#)]
40. Liu, L.; Xu, J.; Yang, J.; Feng, C.; Miao, Y. Imaging human melanoma using a novel Tc- 99m -labeled lactam bridge-cyclized alpha-MSH peptide. *Bioorg. Med. Chem. Lett.* **2016**, *26*, 4724–4728. [[CrossRef](#)]
41. Guo, H.; Miao, Y. Introduction of an 8-amino-octanoic acid linker enhances uptake of ^{99m}Tc -labeled lactam bridge-cyclized α -MSH peptide in melanoma. *J. Nucl. Med.* **2014**, *55*, 2057–2063. [[CrossRef](#)]
42. Aranda-Lara, L.; Ferro-Flores, G.; Isaac-Olivé, K. Improved radiopharmaceutical based on ^{99m}Tc -Bombesin-folate for breast tumour imaging. *Nucl. Med. Commun.* **2016**, *37*, 377–386. [[CrossRef](#)] [[PubMed](#)]
43. Marostica, L.L.; De Barros, A.L.B.; Silva, J.; Oliveira, M.C. Feasibility study with ^{99m}Tc -HYNIC- β Ala-Bombesin(7-14) as an agent to early visualization of lung tumour cells in nude mice. *Nucl. Med. Commun.* **2016**, *37*, 372–376. [[CrossRef](#)] [[PubMed](#)]
44. Mozaffari, S.; Erfani, M.; Beiki, D.; Fallahi, B. Synthesis and preliminary evaluation of a new ^{99m}Tc labeled substance P analogue as a potential tumor imaging agent. *Iran. J. Pharm. Res.* **2015**, *14*, 97–110. [[PubMed](#)]
45. Pach, D.; Sowa-Staszczak, A.; Hubalewska-Dydejczyk, A. Glucagon-like peptide-1 receptor imaging with [Lys⁴⁰(Ahx-HYNIC- ^{99m}Tc /EDDA)NH₂]-exendin-4 for the diagnosis of recurrence or dissemination of medullary thyroid cancer. *Int. J. Endocrinol.* **2013**, *2013*, 384508. [[CrossRef](#)]
46. Altıparmak, B.; Lambrecht, F.Y.; Er, O. Design of ^{99m}Tc -DTPA-CLP and preliminary evaluation in rats. *Chem. Biol. Drug Des.* **2014**, *83*, 362–366. [[CrossRef](#)]
47. Van Domselaar, G.H.; Okarvi, S.M.; Fanta, M.; Suresh, M.R.; Wishart, D.S. Synthesis and ^{99m}Tc -labelling of bz-MAG₃-triprolynyl-peptides, their radiochemical evaluation and in vitro receptor-binding. *J. Label. Compd. Radiopharm.* **2000**, *43*, 1193–1204. [[CrossRef](#)]
48. Gandomkar, M.; Najafi, R.; Babaei, M.H.; Shafiei, M.; Ebrahimi, S.E.S. Synthesis, development and preclinical comparison of two new peptide based freeze-dried kit formulation ^{99m}Tc -EDDA-Tricine-HYNIC-TOC and ^{99m}Tc -EDDA-Tricine-HYNIC-TATE for somatostatin receptor positive tumor scintigraphy. *DARU* **2006**, *14*, 183–189.
49. Wadas, T.J.; Wong, E.H.; Weisman, G.R.; Anderson, C.J. Coordinating Radiometals of Copper, Gallium, Indium, Yttrium and Zirconium for PET and SPECT Imaging of Disease. *Chem. Rev.* **2010**, *110*, 2858–2902. [[CrossRef](#)]
50. Meyer, G.J.; Mäcke, H.; Schuhmacher, J.; Knapp, W.H.; Hofmann, M. ^{68}Ga -labelled DOTA-derivatised peptide ligands. *Eur. J. Nucl. Med. Mol. Imaging* **2004**, *31*, 1097–1104. [[CrossRef](#)] [[PubMed](#)]
51. Ambrosini, V.; Campana, D.; Tomassetti, P.; Fanti, S. ^{68}Ga -labelled peptides for diagnosis of gastroenteropancreatic NET. *Eur. J. Nucl. Med. Mol. Imaging* **2012**, *39*, 52–60. [[CrossRef](#)]
52. Eisenwiener, K.P.; Prata, M.I.M.; Buschmann, I.; Mäcke, H.R. NODAGATOC, a new chelator-coupled somatostatin analogue labeled with [$^{67/68}\text{Ga}$] and [^{111}In] for SPECT, PET, and targeted therapeutic applications of somatostatin receptor (hsst2) expressing tumors. *Bioconj. Chem.* **2002**, *13*, 530–541. [[CrossRef](#)] [[PubMed](#)]
53. Sinnes, J.P.; Bauder-Wuest, U.; Schäfer, M.; Roesch, F. ^{68}Ga , ^{44}Sc and ^{177}Lu -labeled AAZTA5-PSMA-617: Synthesis, radiolabeling, stability and cell binding compared to DOTA-PSMA-617 analogues. *EJNMMI Radiopharm. Chem.* **2020**, *5*, 28. [[CrossRef](#)] [[PubMed](#)]
54. Eder, M.; Wängler, B.; Knackmuss, S.; Eisenhut, M. Tetrafluorophenolate of HBED-CC: A versatile conjugation agent for ^{68}Ga -labeled small recombinant antibodies. *Eur. J. Nucl. Med. Mol. Imaging* **2008**, *35*, 1878–1886. [[CrossRef](#)]
55. Afshar-Oromieh, A.; Malcher, A.; Eder, M.; Zechmann, C.M. PET imaging with a [^{68}Ga]gallium-labelled PSMA ligand for the diagnosis of prostate cancer: Biodistribution in humans and first evaluation of tumour lesions. *Eur. J. Nucl. Med. Mol. Imaging* **2013**, *40*, 486–495. [[CrossRef](#)]
56. Notni, J.; Hermann, P.; Havlickova, J.; Lukes, I. A Triazacyclononane-Based Bifunctional Phosphinate Ligand for the Preparation of Multimeric ^{68}Ga Tracers for Positron Emission Tomography. *Chem. Eur. J.* **2010**, *16*, 7174–7185. [[CrossRef](#)]
57. Ma, M.T.; Cullinane, C.; Imberti, C.; Blower, P.J. New Tris(hydroxypyridinone) Bifunctional Chelators Containing Isothiocyanate Groups Provide a Versatile Platform for Rapid One-Step Labeling and PET Imaging with $^{68}\text{Ga}^{3+}$. *Bioconj. Chem.* **2016**, *27*, 309–318. [[CrossRef](#)] [[PubMed](#)]
58. Liu, B.; Zhang, Z.; Wang, H.; Yao, S. Preclinical evaluation of a dual sstr2 and integrin $\alpha_v\beta_3$ -targeted heterodimer [^{68}Ga]-NOTA-3PEG₄-TATE-RGD. *Bioorg. Med. Chem.* **2019**, *27*, 115094. [[CrossRef](#)]
59. Lamarca, A.; Pritchard, D.M.; Westwood, T.; Mansoor, W. ^{68}Ga Gallium DOTANOC-PET Imaging in Lung Carcinoids: Impact on Patients' Management. *Neuroendocrinology* **2018**, *106*, 128–138. [[CrossRef](#)] [[PubMed](#)]
60. Nicolas, G.P.; Schreiter, N.; Kaul, F.; Wild, D. Sensitivity comparison of ^{68}Ga -OPS202 and ^{68}Ga -DOTATOC PET/CT in patients with gastroenteropancreatic neuroendocrine tumors: A prospective phase II imaging study. *J. Nucl. Med.* **2018**, *59*, 915–921. [[CrossRef](#)]

61. Eder, M.; Schäfer, M.; Bauder-Wuest, U.; Kopka, K. Preclinical evaluation of a bispecific low-molecular heterodimer targeting both PSMA and GRPR for improved PET imaging and therapy of prostate cancer. *Prostate* **2014**, *74*, 659–668. [[CrossRef](#)]
62. Verburg, F.A.; Krohn, T.; Heinzl, A.; Mottaghy, F.M.; Behrendt, F.F. First evidence of PSMA expression in differentiated thyroid cancer using [^{68}Ga] PSMA-HBED-CC PET/CT. *Eur. J. Nucl. Med. Mol. Imaging* **2015**, *42*, 1622–1623. [[CrossRef](#)] [[PubMed](#)]
63. Heppeler, A.; Froidevaux, S.; Eberle, A.N.; Mäcke, H.R. Receptor Targeting for Tumor Localisation and Therapy with Radiopetides. *Curr. Med. Chem.* **2000**, *7*, 971–994. [[CrossRef](#)]
64. Virgolini, I.; Britton, K.; Buscombe, J.; Riva, P. ^{111}In - and ^{90}Y -DOTA-lanreotide: Results and implications of the MAURITIUS trial. *Semin. Nucl. Med.* **2002**, *32*, 148–155. [[CrossRef](#)] [[PubMed](#)]
65. Garrison, J.C.; Rold, T.L.; Sieckman, G.L.; Hoffman, T.J. Evaluation of the pharmacokinetic effects of various linking group using the ^{111}In -DOTA-X-BBN(7-14) NH_2 structural paradigm in a prostate cancer model. *Bioconj. Chem.* **2008**, *19*, 1803–1812. [[CrossRef](#)]
66. Breeman, W.A.P.; Hofland, L.J.; Van der Pluijm, M.; Krenning, E.P. A new radiolabelled somatostatin analogue [^{111}In -DTPA-D-Phe 1]RC-160: Preparation, biological activity, receptor scintigraphy in rats and comparison with [^{111}In -DTPA-D-Phe 1]octreotide. *Eur. J. Nucl. Med.* **1994**, *21*, 328–335. [[CrossRef](#)]
67. Joosten, L.; Brom, M.; Peeters, H.; Gotthardt, M. Enhanced Specific Activity by Multichelation of Exendin-3 Leads to Improved Image Quality and in vivo Beta Cell Imaging. *Mol. Pharm.* **2018**, *15*, 486–494. [[CrossRef](#)]
68. Kaeppli, S.A.M.; Jodal, A.; Gotthardt, M.; Schibli, R.; Béhé, M. Exendin-4 Derivatives with an Albumin-Binding Moiety Show Decreased Renal Retention and Improved GLP-1 Receptor Targeting. *Mol. Pharm.* **2019**, *16*, 3760–3769. [[CrossRef](#)]
69. Schollhammer, R.; Gallerande, H.D.C.; Yacoub, M.; Morgat, C. Comparison of the radiolabeled PSMA-inhibitor ^{111}In -PSMA-617 and the radiolabeled GRP-R antagonist ^{111}In -RM2 in primary prostate cancer samples. *EJNMMI Res.* **2019**, *9*, 52. [[CrossRef](#)]
70. Sartori, A.; Bianchini, F.; Migliari, S.; Battistini, L. Synthesis and preclinical evaluation of a novel, selective ^{111}In -labelled aminoproline-RGD-peptide for non-invasive melanoma tumor imaging. *Med. Chem. Commun.* **2015**, *6*, 2175–2183. [[CrossRef](#)]
71. Anderson, C.J.; Ferdani, R. Copper-64 radiopharmaceuticals for PET imaging of cancer: Advances in preclinical and clinical research. *Cancer Biother. Radiopharm.* **2009**, *24*, 379–393. [[CrossRef](#)]
72. Dale, A.V.; An, G.I.; Pandya, D.N.; Yoo, J. Synthesis and Evaluation of New Generation Cross-Bridged Bifunctional Chelator for ^{64}Cu Radiotracers. *Inorg. Chem.* **2015**, *54*, 8177–8186. [[CrossRef](#)] [[PubMed](#)]
73. Mansour, N.; Paquette, M.; Ait-Mohand, S.; Dumulon-Perreault, V.; Guérin, B. Evaluation of a novel GRPR antagonist for prostate cancer PET imaging: [^{64}Cu]-DOTHA $_2$ -PEG-RM26. *Nucl. Med. Biol.* **2018**, *56*, 31–38. [[CrossRef](#)]
74. Lucente, E.; Liu, H.; Liu, Y.; Cheng, Z. Novel ^{64}Cu Labeled RGD $_2$ -BBN Heterotrimers for PET Imaging of Prostate Cancer. *Bioconj. Chem.* **2018**, *29*, 1595–1604. [[CrossRef](#)]
75. Chen, X.; Liu, S.; Hou, Y.; Conti, P.S. MicroPET imaging of breast cancer α_v -integrin expression with ^{64}Cu -labeled dimeric RGD peptides. *Mol. Imaging Biol.* **2004**, *6*, 350–359. [[CrossRef](#)]
76. Jin, Z.H.; Furukawa, T.; Galibert, M.; Fujibayashi, Y. Noninvasive visualization and quantification of tumor $\alpha_v\beta_3$ integrin expression using a novel positron emission tomography probe, ^{64}Cu -cyclam-RAFT-c(-RGDFK)- $_4$. *Nucl. Med. Biol.* **2011**, *38*, 529–540. [[CrossRef](#)]
77. Kelly, J.M.; Ponnala, S.; Amor-Coarasa, A.; Babich, J.W. Preclinical Evaluation of a High-Affinity Sarcophagine-Containing PSMA Ligand for $^{64}\text{Cu}/^{67}\text{Cu}$ -Based Theranostics in Prostate Cancer. *Mol. Pharm.* **2020**, *17*, 1954–1962. [[CrossRef](#)] [[PubMed](#)]
78. Craft, J.M.; De Silva, R.A.; Lears, K.A.; Rogers, B.E. In vitro and in vivo evaluation of a ^{64}Cu -labeled NOTA-Bn-SCN-Aoc-bombesin analogue in gastrin-releasing peptide receptor expressing prostate cancer. *Nucl. Med. Biol.* **2012**, *39*, 609–616. [[CrossRef](#)]
79. Fournier, P.; Dumulon-Perreault, V.; Ait-Mohand, S.; Guerin, B. Novel radiolabeled peptides for breast and prostate tumor PET imaging: ^{64}Cu /and ^{68}Ga /NOTA-PEG-[D-Tyr 6 , β Ala 11 ,Thi 13 ,Nle 14]BBN(6-14). *Bioconj. Chem.* **2012**, *23*, 1687–1693. [[CrossRef](#)]
80. Banerjee, S.R.; Pullambhatla, M.; Foss, C.A.; Pomper, M.G. ^{64}Cu -labeled inhibitors of prostate-specific membrane antigen for PET imaging of prostate cancer. *J. Med. Chem.* **2014**, *57*, 2657–2669. [[CrossRef](#)] [[PubMed](#)]
81. Green, M.A.; Mathias, C.J.; Willis, L.R.; Hutchins, G.D. Assessment of Cu-ETS as a PET radiopharmaceutical for evaluation of regional renal perfusion. *Nucl. Med. Biol.* **2007**, *34*, 247–255. [[CrossRef](#)] [[PubMed](#)]
82. Liu, J.; Hajibeigi, A.; Ren, G.; Oz, O.K. Retention of the radiotracers ^{64}Cu -ATSM and ^{64}Cu -PTSM in human and murine tumors is influenced by MDR1 protein expression. *J. Nucl. Med.* **2009**, *50*, 1332–1339. [[CrossRef](#)] [[PubMed](#)]
83. Lewis, J.S.; Srinivasan, A.; Schmidt, M.A.; Anderson, C.J. In vitro and in vivo evaluation of ^{64}Cu -TETA-Tyr 3 -octreotate. A new somatostatin analog with improved target tissue uptake. *Nucl. Med. Biol.* **1999**, *26*, 267–273. [[CrossRef](#)]
84. Pandya, D.N.; Kim, J.Y.; Kwak, W.; Park, C.J.; Yoo, J. A New Synthesis of TE2A—A Potential Bifunctional Chelator for ^{64}Cu . *Nucl. Med. Mol. Imaging* **2010**, *44*, 185–192. [[CrossRef](#)] [[PubMed](#)]
85. Di Bartolo, N.M.; Sargeson, A.M.; Donlevy, T.M.; Smith, S.V. Synthesis of a new cage ligand, SarAr, and its complexation with selected transition metal ions for potential use in radioimaging. *J. Chem. Soc. Dalton Trans.* **2001**, 2303–2309. [[CrossRef](#)]
86. Deri, M.A.; Zeglis, B.M.; Francesconi, L.C.; Lewis, J.S. PET Imaging with ^{89}Zr : From Radiochemistry to the Clinic. *Nucl. Med. Biol.* **2013**, *40*, 3–14. [[CrossRef](#)]
87. Ekberg, C.; Källvenius, G.; Albinsson, Y.; Brown, P.L. Studies on the hydrolytic behavior of zirconium(IV). *J. Solut. Chem.* **2004**, *33*, 47–79. [[CrossRef](#)]
88. McKnight, B.N.; Viola-Villegas, N.T. ^{89}Zr -ImmunoPET Companion Diagnostics and their Impact in Clinical Drug Development. *J. Label. Compd. Radiopharm.* **2018**, *61*, 727–738. [[CrossRef](#)]

89. Noor, A.; Van Zuylekom, J.K.; Rudd, S.E.; Donnelly, P.S. Bivalent Inhibitors of Prostate-Specific Membrane Antigen Conjugated to Desferrioxamine B Squaramide Labeled with Zirconium-89 or Gallium-68 for Diagnostic Imaging of Prostate Cancer. *J. Med. Chem.* **2020**, *63*, 9258–9270. [[CrossRef](#)]
90. Tinianow, J.N.; Pandya, D.N.; Pailloux, S.L.; Marik, J. Evaluation of a 3-hydroxypyridin-2-one (2,3-HOPO) Based Macrocyclic Chelator for $^{89}\text{Zr}^{4+}$ and Its Use for ImmunoPET Imaging of HER2 Positive Model of Ovarian Carcinoma in Mice. *Theranostics* **2016**, *6*, 511–521. [[CrossRef](#)]
91. Vugts, D.J.; Van Dongen, G.A.M.S. ^{89}Zr -labeled compounds for PET imaging guided personalized therapy. *Drug Discov. Today Technol.* **2011**, *8*, e53–e61. [[CrossRef](#)] [[PubMed](#)]
92. Kolb, H.C.; Finn, M.G.; Sharpless, K.B. Click Chemistry: Diverse Chemical Function from a Few Good Reactions. *Angew. Chem. Int. Ed. Engl.* **2001**, *40*, 2004–2021. [[CrossRef](#)]
93. Nwe, K.; Brechbiel, M.W. Growing Applications of “Click Chemistry” for Bioconjugation in Contemporary Biomedical Research. *Cancer Biother. Radiopharm.* **2009**, *24*, 289–302. [[CrossRef](#)]
94. Mindt, T.; Struthers, H.; Brans, L.; Schibli, R. “Click to Chelate”: Synthesis and Installation of Metal Chelates into Biomolecules in a Single Step. *J. Am. Chem. Soc.* **2006**, *128*, 15096–15097. [[CrossRef](#)]
95. Struthers, H.; Spingler, B.; Mindt, T.L.; Schibli, R. “Click-to-Chelate”: Design and Incorporation of Triazole-Containing Metal-Chelating Systems into Biomolecules of Diagnostic and Therapeutic Interest. *Chem. Eur. J.* **2008**, *14*, 6173–6183. [[CrossRef](#)]
96. Mushtaq, S.; Yun, S.J.; Jeon, J. Recent Advances in Bioorthogonal Click Chemistry for Efficient Synthesis of Radiotracers and Radiopharmaceuticals. *Molecules* **2019**, *24*, 3567. [[CrossRef](#)] [[PubMed](#)]
97. Svatunek, D.; Houszka, N.; Hamlin, T.A.; Bickelhaupt, F.M.; Mikula, H. Chemoselectivity of Tertiary Azides in Strain-Promoted Alkyne-Azide Cycloadditions. *Chem. Eur. J.* **2019**, *25*, 754–758. [[CrossRef](#)] [[PubMed](#)]
98. Kasten, B.B.; Ma, X.; Liu, H.; Benny, P.D. Clickable, hydrophilic ligand for $\text{fac}[\text{M}^{\text{I}}(\text{CO})_3]^+$ ($\text{M} = \text{Re}/^{99\text{m}}\text{Tc}$) applied in an S-functionalized α -MSH peptide. *Bioconj. Chem.* **2014**, *25*, 579–592. [[CrossRef](#)] [[PubMed](#)]
99. Castillo Gomez, J.D.; Hagenbach, A.; Abram, U. Propargyl-Substituted Thiocarbamoylbenzamidines of Technetium and Rhenium: Steps towards Bioconjugation with Use of Click Chemistry. *Eur. J. Inorg. Chem.* **2016**, *2016*, 5427–5434. [[CrossRef](#)]
100. Connell, T.U.; Hayne, D.J.; Ackermann, U.; Donnelly, P.S. Rhenium and technetium tricarbonyl complexes of 1,4-Substituted pyridyl-1,2,3-triazole bidentate ‘click’ ligands conjugated to a targeting RGD peptide. *J. Label. Compd. Radiopharm.* **2014**, *57*, 262–269. [[CrossRef](#)]
101. Wängler, C.; Schäfer, M.; Schirmmayer, R.; Bartenstein, P.; Wängler, B. DOTA derivatives for site-specific biomolecule-modification via click chemistry. *Bioorg. Med. Chem.* **2011**, *19*, 3864–3874. [[CrossRef](#)]
102. Martin, M.E.; O’Dorisio, S.M.; Leverich, W.M.; Kloepping, K.C.; Schultz, M.K. “Click”-Cyclized ^{68}Ga -Labeled peptides for molecular imaging and therapy: Synthesis and preliminary in vitro and in vivo evaluation in a melanoma model system. *Recent Results Cancer Res.* **2013**, *194*, 149–175. [[CrossRef](#)]
103. Baumhover, N.J.; Martin, M.E.; Parameswarappa, S.G.; Schultz, M.K. Improved synthesis and biological evaluation of chelator-modified α -MSH analogues prepared by copper-free click chemistry. *Bioorg. Med. Chem. Lett.* **2011**, *21*, 5757–5761. [[CrossRef](#)] [[PubMed](#)]
104. Nakamoto, Y.; Pradipta, A.R.; Mukai, H.; Tanaka, K. Expanding the Applicability of the Metal Labeling of Biomolecules by the RIKEN Click Reaction: A Case Study with Gallium-68 Positron Emission Tomography. *ChemBioChem* **2018**, *19*, 2055–2060. [[CrossRef](#)] [[PubMed](#)]
105. Evans, H.L.; Carroll, L.; Aboagye, E.O.; Spivey, A.C. Bioorthogonal chemistry for ^{68}Ga radiolabelling of DOTA-containing compounds. *J. Label. Compd. Radiopharm.* **2014**, *57*, 291–297. [[CrossRef](#)]
106. Makarem, A.; Sarvestani, M.K.; Klika, K.D.; Kopka, K. A Multifunctional HBED-Type Chelator with Dual Conjugation Capabilities for Radiopharmaceutical Development. *Synlett* **2019**, *30*. [[CrossRef](#)]
107. Kaeopookum, P.; Petrik, M.; Summer, D.; Decristoforo, C. Comparison of ^{68}Ga -labeled RGD mono- and multimers based on a clickable siderophore-based scaffold. *Nucl. Med. Biol.* **2019**, *78–79*, 1–10. [[CrossRef](#)] [[PubMed](#)]
108. Baranyai, Z.; Reich, D.; Vagner, A.; Notni, J. A shortcut to high-affinity Ga-68 and Cu-64 radiopharmaceuticals: One-pot click chemistry trimerisation on the TRAP platform. *Dalton Trans.* **2015**, *44*, 11137–11146. [[CrossRef](#)]
109. Quigley, N.G.; Tomassi, S.; Di Leva, F.S.; Notni, J. Click-Chemistry (CuAAC) Trimerization of an $\alpha_v\beta_6$ Integrin Targeting Ga-68-Peptide: Enhanced Contrast for in-Vivo PET Imaging of Human Lung Adenocarcinoma Xenografts. *ChemBioChem* **2020**, *21*, 2836–2843. [[CrossRef](#)]
110. Notni, J.; Reich, D.; Maltsev, O.V.; Wester, H.J. In Vivo PET imaging of the cancer integrin $\alpha_v\beta_6$ using ^{68}Ga -labeled cyclic RGD nonapeptides. *J. Nucl. Med.* **2017**, *58*, 671–677. [[CrossRef](#)]
111. Radford, L.L.; Papagiannopoulou, D.; Gallazzi, F.; Hennkens, H.M. Synthesis and evaluation of $\text{Re}/^{99\text{m}}\text{Tc}(\text{I})$ complexes bearing a somatostatin receptor-targeting antagonist and labeled via a novel [N,S,O] clickable bifunctional chelating agent. *Bioorg. Med. Chem.* **2019**, *27*, 492–501. [[CrossRef](#)] [[PubMed](#)]
112. Summer, D.; Mayr, S.; Petrik, M.; Decristoforo, C. Pretargeted Imaging with Gallium-68—Improving the Binding Capability by Increasing the Number of Tetrazine Motifs. *Pharmaceuticals* **2018**, *11*, 102. [[CrossRef](#)] [[PubMed](#)]
113. Chen, K.T.; Nguyen, K.; Ieritano, C.; Gao, F.; Seimbille, Y. A Flexible Synthesis of ^{68}Ga -Labeled Carbonic Anhydrase IX (CAIX)-Targeted Molecules via CBT/1,2-Amino-thiol Click Reaction. *Molecules* **2019**, *24*, 23. [[CrossRef](#)] [[PubMed](#)]
114. Ge, J.; Zhang, Q.; Zeng, J.; Gu, Z.; Gao, M. Radiolabeling nanomaterials for multimodality imaging: New insights into nuclear medicine and cancer diagnosis. *Biomaterials* **2020**, *228*, 119553. [[CrossRef](#)]

115. Farzin, L.; Sheibani, S.; Moassesi, M.E.; Shamsipur, M. An overview of nanoscale radionuclides and radiolabeled nanomaterials commonly used for nuclear molecular imaging and therapeutic functions. *J. Biomed. Mater. Res. A* **2019**, *107*, 251–285. [[CrossRef](#)]
116. Varani, M.; Galli, F.; Auletta, S.; Signore, A. Radiolabelled nanoparticles for cancer diagnosis. *Clin. Transl. Imaging* **2018**, *6*, 271–292. [[CrossRef](#)]
117. Koziorowski, J.; Stanciu, A.E.; Gomez-Vallejo, V.; Llop, J. Radiolabeled nanoparticles for cancer diagnosis and therapy. *AntiCancer Agents Med. Chem.* **2017**, *17*, 333–354. [[CrossRef](#)] [[PubMed](#)]
118. Wall, M.; Schäffer, T.M.; Harmsen, S.; Kircher, M. Chelator-Free Radiolabeling of SERRS Nanoparticles for Whole-Body PET and Intraoperative Raman Imaging. *Theranostics* **2017**, 3068–3077. [[CrossRef](#)] [[PubMed](#)]
119. Morales-Avila, E.; Ferro-Flores, G.; Gomez-Olivan, L. Multimeric system of ^{99m}Tc -labeled gold nanoparticles conjugated to c[RGDFK(C)] for molecular imaging of tumor $\alpha(v)\beta(3)$ expression. *Bioconj. Chem.* **2011**, *22*, 913–922. [[CrossRef](#)]
120. Peiris, P.M.; Deb, P.; Doolittle, E.; Karathanasis, E. Vascular targeting of a gold nanoparticle to breast cancer metastasis. *J. Pharm. Sci.* **2015**, *104*, 2600–2610. [[CrossRef](#)] [[PubMed](#)]
121. Mendoza-Sanchez, A.N.; Ferro-Flores, G.; Camacho-Lopez, M.A. Lys3-bombesin conjugated to ^{99m}Tc -labelled gold nanoparticles for in vivo gastrin releasing peptide-receptor imaging. *J. Biomed. Nanotechnol.* **2010**, *6*, 375–384. [[CrossRef](#)]
122. Silva, F.; Gano, L.; Campello, M.P.C.; Kannan, R. In vitro/in vivo “peeling” of multilayered aminocarboxylate gold nanoparticles evidenced by a kinetically stable ^{99m}Tc -label. *Dalton Trans.* **2017**, *46*, 14572–14583. [[CrossRef](#)] [[PubMed](#)]
123. Orocio-Rodriguez, E.; Ferro-Flores, G.; Sanchez-Garcia, F.M. Two novel nanosized radiolabeled analogues of somatostatin for neuroendocrine tumor imaging. *J. Nanosci. Nanotechnol.* **2015**, *15*, 4159–4169. [[CrossRef](#)] [[PubMed](#)]
124. Braga, T.L.; Pinto, S.R.; Reis, S.R.R.; Santos-Oliveira, R. Octreotide Nanoparticles Showed Affinity for in vivo MIA Paca-2 Induced Pancreas Ductal Adenocarcinoma Mimicking Pancreatic Polypeptide-Secreting Tumor of the Distal Pancreas (PPoma). *Pharm. Res.* **2019**, *36*, 143. [[CrossRef](#)]
125. Ng, Q.K.T.; Olariu, C.I.; Yaffee, M.; Walter, M.A. Indium-111 labeled gold nanoparticles for in-vivo molecular targeting. *Biomaterials* **2014**, *35*, 7050–7057. [[CrossRef](#)] [[PubMed](#)]
126. Rangger, C.; Helbok, A.; Sosabowski, J.; Decristoforo, C. Tumor targeting and imaging with dual-peptide conjugated multifunctional liposomal nanoparticles. *Int. J. Nanomed.* **2013**, *8*, 4659–4671. [[CrossRef](#)]
127. Xiao, Y.; Hong, H.; Matson, V.Z.; Gong, S. Gold Nanorods Conjugated with Doxorubicin and cRGD for Combined Anticancer Drug Delivery and PET Imaging. *Theranostics* **2012**, *2*, 757–768. [[CrossRef](#)] [[PubMed](#)]
128. Cai, H.; Xie, F.; Mulgaonkar, A.; Wu, C.; Ai, H. Bombesin functionalized ^{64}Cu -copper sulfide nanoparticles for targeted imaging of orthotopic prostate cancer. *Nanomedicine* **2018**, *13*, 1695–1705. [[CrossRef](#)]
129. Chilug, L.E.; Leonte, R.A.; Patrascu, M.E.B.; Niculae, D. In vitro binding kinetics study of gold nanoparticles functionalized with ^{68}Ga -DOTA conjugated peptides. *J. Radioanal. Nucl. Chem.* **2017**, *311*, 1485–1493. [[CrossRef](#)]
130. Lahooti, A.; Shانهsazzadeh, S.; Laurent, S. Preliminary studies of ^{68}Ga -NODA-USPION-BBN as a dual-modality contrast agent for use in positron emission tomography/magnetic resonance imaging. *Nanotechnology* **2020**, *31*, 015102. [[CrossRef](#)]
131. Hajiramezanali, M.; Atyabi, F.; Mosayebnia, M.; Beiki, D. ^{68}Ga -radiolabeled bombesin-conjugated to trimethyl chitosan-coated superparamagnetic nanoparticles for molecular imaging: Preparation, characterization and biological evaluation. *Int. J. Nanomed.* **2019**, *14*, 2591–2605. [[CrossRef](#)] [[PubMed](#)]
132. Cuccurullo, V.; Prisco, M.R.; Di Stasio, G.D.; Mansi, L. Nuclear Medicine in Patients with NET: Radiolabeled Somatostatin Analogues and their Brothers. *Curr. Radiopharm.* **2017**, *10*, 74–84. [[CrossRef](#)] [[PubMed](#)]
133. Cakir, M.; Dworakowska, D.; Grossman, A. Somatostatin receptor biology in neuroendocrine and pituitary tumours: Part 2—Clinical implications. *J. Cell. Mol. Med.* **2010**, *14*, 2585–2591. [[CrossRef](#)] [[PubMed](#)]
134. Orlando, C.; Raggi, C.C.; Bianchi, S.; Serio, M. Measurement of somatostatin receptor subtype 2 mRNA in breast cancer and corresponding normal tissue. *Endocr. Relat. Cancer* **2004**, *11*, 323–332. [[CrossRef](#)] [[PubMed](#)]
135. Lapa, C.; Häscheid, H.; Wild, V.; Lückerrath, K. Somatostatin receptor expression in small cell lung cancer as a prognostic marker and a target for peptide receptor radionuclide therapy. *Oncotarget* **2016**, *7*, 20033–20040. [[CrossRef](#)] [[PubMed](#)]
136. Lum, S.S.; Fletcher, W.S.; O’Dorisio, M.S.; Caprara, M. Distribution and functional significance of somatostatin receptors in malignant melanoma. *World J. Surg.* **2001**, *25*, 407–412. [[CrossRef](#)]
137. Liu, Q.; Cescato, R.; Dewi, D.A.; Schonbrunn, A. Receptor signaling and endocytosis are differentially regulated by somatostatin analogues. *Mol. Pharmacol.* **2005**, *68*, 90–101. [[CrossRef](#)]
138. Janssen, I.; Chen, C.C.; Taieb, D.; Pacak, K. ^{68}Ga -DOTATATE PET/CT in the Localization of Head and Neck Paragangliomas Compared with Other Functional Imaging Modalities and CT/MRI. *J. Nucl. Med.* **2016**, *57*, 186–191. [[CrossRef](#)]
139. Basu, S.; Ranade, R.; Hazarik, S. ^{68}Ga DOTATATE PET/CT of Synchronous Meningioma and Prolactinoma. *Clin. Nucl. Med.* **2016**, *41*, 230. [[CrossRef](#)] [[PubMed](#)]
140. Binse, I.; Poeppel, T.D.; Ruhlmann, M.; Krumme, S.J.R. ^{68}Ga -DOTATOC PET/CT in Patients with Iodine- and 18F-FDG-Negative Differentiated Thyroid Carcinoma and Elevated Serum Thyroglobulin. *J. Nucl. Med.* **2016**, *57*, 1512–1517. [[CrossRef](#)]
141. Walker, R.; Deppen, S.; Smith, G.; Massion, P.P. ^{68}Ga -DOTATATE PET/CT imaging of indeterminate pulmonary nodules and lung cancer. *PLoS ONE* **2017**, *12*, e0171301. [[CrossRef](#)]
142. Ilan, E.; Sandstrom, M.; Velikyan, I.; Sundin, A.; Eriksson, B.; Lubberink, M. Parametric Net Influx Rate Images of ^{68}Ga -DOTATOC and ^{68}Ga -DOTATATE: Quantitative Accuracy and Improved Image Contrast. *J. Nucl. Med.* **2017**, *58*, 744–749. [[CrossRef](#)] [[PubMed](#)]

143. Abiraj, K.; Ursillo, S.; Tamma, M.L.; Mäcke, H.R. The tetraamine chelator outperforms HYNIC in a new technetium-99m-labelled somatostatin receptor 2 antagonist. *EJNMMI Res.* **2018**, *8*, 75. [CrossRef]
144. Liu, F.; Liu, T.; Xu, X.; Yang, Z. Design, Synthesis, and Biological Evaluation of ⁶⁸Ga-DOTA-PA1 for Lung Cancer: A Novel PET Tracer for Multiple Somatostatin Receptor Imaging. *Mol. Pharm.* **2018**, *15*, 619–628. [CrossRef]
145. Rylova, S.; Stoykow, C.; Del Pozzo, L.; Mäcke, H.R. The somatostatin receptor 2 antagonist ⁶⁴Cu-NODAGA-JR11 outperforms ⁶⁴Cu-DOTA-TATE in a mouse xenograft model. *PLoS ONE* **2018**, *13*, e0195802. [CrossRef]
146. Mukherjee, A.; Korde, A.; Shinto, A.; Dash, A. Studies on batch formulation of a freeze dried kit for the preparation of ^{99m}Tc-HYNIC-TATE for imaging neuroendocrine tumors. *Appl. Radiat. Isot.* **2019**, *145*, 180–186. [CrossRef] [PubMed]
147. Mapelli, P.; Ironi, G.; Fallanca, F.; Picchio, M. ⁶⁸Ga-DOTA-peptides PET/MRI in pancreatico-duodenal neuroendocrine tumours: A flash pictorial essay on assets and lacks. *Clin. Transl. Imaging* **2019**, *7*, 363–371. [CrossRef]
148. Yadav, D.; Ballal, S.; Yadav, M.P.; Tripathi, M.; Roesch, F.; Bal, C. Evaluation of [⁶⁸Ga]Ga-DOTA-TOC for imaging of neuroendocrine tumours: Comparison with [⁶⁸Ga]Ga-DOTA-NOC PET/CT. *Eur. J. Nucl. Med. Mol. Imaging* **2020**, *47*, 860–869. [CrossRef] [PubMed]
149. Moreno, P.; Ramos-Alvarez, I.; Moody, T.W.; Jensen, R.T. Bombesin related peptides/receptors and their promising therapeutic roles in cancer imaging, targeting and treatment. *Expert Opin. Ther. Targets* **2016**, *20*, 1055–1073. [CrossRef]
150. Baidoo, K.E.; Lin, K.S.; Zhan, Y.; Wagner, H.N. Design, synthesis, and initial evaluation of high-affinity technetium bombesin analogues. *Bioconj. Chem.* **1998**, *9*, 218–225. [CrossRef] [PubMed]
151. Baratto, L.; Jadvar, H.; Jagaru, A. Prostate Cancer Theranostics Targeting Gastrin-Releasing Peptide Receptors. *Mol. Imaging Biol.* **2017**, *20*, 501–509. [CrossRef]
152. Nock, B.A.; Kaloudi, A.; Lymperis, E.; Maina, T.; Baum, R.P. Theranostic Perspectives in Prostate Cancer with the Gastrin-Releasing Peptide Receptor Antagonist NeobOMB1: Preclinical and First Clinical Results. *J. Nucl. Med.* **2017**, *58*, 75–80. [CrossRef]
153. Mitran, B.; Thisgaard, H.; Rosenstrom, U.; Orlova, A. High Contrast PET Imaging of GRPR Expression in Prostate Cancer Using Cobalt-Labeled Bombesin Antagonist RM26. *Contrast Media Mol. Imaging* **2017**, *2017*, 6873684. [CrossRef]
154. Mendoza-Figueroa, M.J.; Escudero-Castellanos, A.; Ramirez-Nava, G.J.; Avila-Rodriguez, M.A. Preparation and preclinical evaluation of ⁶⁸Ga-iPSMA-BN as a potential heterodimeric radiotracer for PET-imaging of prostate cancer. *J. Radioanal. Nucl. Chem.* **2018**, *318*, 2097–2105. [CrossRef]
155. Touijer, K.A.; Michaud, L.; Vargas Alvarez, H.A.; Weber, W.A. Prospective Study of the Radiolabeled GRPR Antagonist BAY86-7548 for Positron Emission Tomography/Computed Tomography Imaging of Newly Diagnosed Prostate Cancer. *Eur. Urol. Oncol.* **2019**, *2*, 166–173. [CrossRef]
156. Okarvi, S.M.; Aijammaz, I. A convenient and efficient total solid-phase synthesis of DOTA-functionalized tumor-targeting peptides for PET imaging of cancer. *EJNMMI Res.* **2019**, *9*, 88. [CrossRef]
157. Kanellopoulos, P.; Lymperis, E.; Kaloudi, A.; De Jong, M.; Krenning, E.P.; Nock, B.A.; Maina, T. [^{99m}Tc]Tc-DB1 Mimics with Different-Length PEG Spacers: Preclinical Comparison in GRPR-Positive Models. *Molecules* **2020**, *25*, 3418. [CrossRef]
158. Ferguson, S.; Wuest, M.; Richter, S.; Wuest, F. A comparative PET imaging study of ^{44g}Sc- and ⁶⁸Ga-labeled bombesin antagonist BBN2 derivatives in breast and prostate cancer models. *Nucl. Med. Biol.* **2020**, *90–91*, 74–83. [CrossRef] [PubMed]
159. Roosenburg, S.; Laverman, P.; Van Delft, F.L.; Boerman, O.C. Radiolabeled CCK/gastrin peptides for imaging and therapy of CCK2 receptor-expressing tumors. *Amino Acids* **2011**, *41*, 1049–1058. [CrossRef] [PubMed]
160. Summer, D.; Rangger, C.; Klinger, M.; Decristoforo, C. Exploiting the Concept of Multivalency with ⁶⁸Ga- and ⁸⁹Zr-Labelled Fusarinine C-Minigastrin Bioconjugates for Targeting CCK2R Expression. *Contrast Media Mol. Imaging* **2018**, *2018*, 3171794. [CrossRef] [PubMed]
161. Klinger, M.; Decristoforo, C.; Rangger, C.; Von Guggenberg, E. Site-specific stabilization of minigastrin analogues against enzymatic degradation for enhanced cholecystokinin-2 receptor targeting. *Theranostics* **2018**, *8*, 2896–2908. [CrossRef]
162. Klinger, M.; Rangger, C.; Summer, D.; Von Guggenberg, E. Cholecystokinin-2 Receptor Targeting with Novel C-terminally Stabilized HYNIC-Minigastrin Analogues Radiolabeled with Technetium-99m. *Pharmaceuticals* **2019**, *12*, 13. [CrossRef] [PubMed]
163. Hubalewska-Dydejczyk, A.; Mikolajczak, R.; Decristoforo, C. Radiolabelled CCK-2/Gastrin Receptor Analogue for Personalized Theranostic Strategy in Advanced MTC. 2020; Identifier: NCT03246659. Available online: <https://clinicaltrials.gov/> (accessed on 30 January 2021).
164. Drucker, D.J.; Phillippe, J.; Mojsov, S.; Chick, W.L.; Habener, J.F. Glucagon-like peptide I stimulates insulin gene expression and increases cyclic AMP levels in a rat islet cell line. *Proc. Natl. Acad. Sci. USA* **1987**, *84*, 3434–3438. [CrossRef] [PubMed]
165. Li, M.; Liu, Y.; Xu, Y.; Yang, M. Preliminary evaluation of GLP-1R PET in the diagnosis and risk stratification of pheochromocytomas. *Neoplasma* **2020**, *67*, 27–36. [CrossRef]
166. Michelotti, F.C.; Bowden, G.; Kueppers, A.; Pichler, B.J. PET/MRI enables simultaneous in vivo quantification of β -cell mass and function. *Theranostics* **2020**, *10*, 398–410. [CrossRef] [PubMed]
167. Nieberler, M.; Reuning, U.; Reichart, F.; Kessler, H. Exploring the Role of RGD-Recognizing Integrins in Cancer. *Cancers* **2017**, *9*, 116. [CrossRef]
168. Lobeek, D.; Franssen, G.M.; Ma, M.T.; Rijpkema, M. In vivo characterization of four ⁶⁸Ga-labelled multimeric RGD peptides to image $\alpha_v\beta_3$ integrin expression in two human tumour xenograft mouse models. *J. Nucl. Med.* **2018**, *59*, 1296–1301. [CrossRef] [PubMed]

169. Taira, Y.; Uehara, T.; Tsuchiya, M.; Arano, Y. Coordination-Mediated Synthesis of Purification-Free Bivalent ^{99m}Tc -Labeled Probes for in Vivo Imaging of Saturable System. *Bioconj. Chem.* **2018**, *29*, 459–466. [[CrossRef](#)]
170. Song, Y.S.; Kim, J.H.; Lee, B.C.; Jung, J.H.; Park, H.S.; Kim, S.E. Biodistribution and Internal Radiation Dosimetry of ^{99m}Tc -IDA-D-[c(RGDfK)]₂ (BIK-505), a Novel SPECT Radiotracer for the Imaging of Integrin $\alpha_v\beta_3$ Expression. *Cancer Biother. Radiopharm.* **2018**, *33*, 396–402. [[CrossRef](#)] [[PubMed](#)]
171. Chen, C.J.; Chan, C.H.; Lin, K.L.; Yu, H.M.; Lin, W.J. ^{68}Ga -labelled NOTA-RGD-GE11 peptide for dual integrin and EGFR-targeted tumour imaging. *Nucl. Med. Biol.* **2019**, *68–69*, 22–30. [[CrossRef](#)]
172. Ma, H.; Liu, S.; Zhang, Z.; Su, S. Preliminary biological evaluation of ^{68}Ga -labeled cyclic RGD dimer as an integrin $\alpha_v\beta_3$ -targeting radiotracer for tumor PET imaging. *J. Radioanal. Nucl. Chem.* **2019**, *321*, 857–865. [[CrossRef](#)]
173. Vatsa, R.; Madaan, S.; Chakraborty, S.; Shukla, J. Clinical evaluation of kit based Tc- 99m -HYNIC-RGD2 for imaging angiogenesis in breast carcinoma patients. *Nucl. Med. Commun.* **2020**, *41*, 1250–1256. [[CrossRef](#)] [[PubMed](#)]
174. Pirooznia, N.; Abdi, K.; Beiki, D.; Geramifar, P. Radiosynthesis, Biological Evaluation, and Preclinical Study of a ^{68}Ga -Labeled Cyclic RGD Peptide as an Early Diagnostic Agent for Overexpressed $\alpha_v\beta_3$ Integrin Receptors in Non-Small-Cell Lung Cancer. *Contrast Media Mol. Imaging* **2020**, *2020*, 8421657. [[CrossRef](#)]
175. Ouyang, Q.; Zhou, J.; Yang, W.; Cui, H.; Xu, M.; Yi, L. Oncogenic role of neurotensin and neurotensin receptors in various cancers. *Clin. Exp. Pharmacol. Physiol.* **2017**, *44*, 841–846. [[CrossRef](#)] [[PubMed](#)]
176. Wolf Horrell, E.M.; Boulanger, M.C.; D’Orazio, J.A. Melanocortin 1 Receptor: Structure, Function, and Regulation. *Front. Genet.* **2016**, *7*, 95. [[CrossRef](#)] [[PubMed](#)]
177. Douglas, S.D.; Leeman, S.E. Neurokinin-1 receptor: Functional significance in the immune system in reference to selected infections and inflammation. *Ann. N. Y. Acad. Sci.* **2011**, *1217*, 83–95. [[CrossRef](#)]
178. Moody, T.W.; Berenguer, B.N.; Jensen, R.T. VIP/PACAP, and their receptors and cancer. *Curr. Opin. Endocrinol. Diabetes Obes.* **2016**, *23*, 38–47. [[CrossRef](#)] [[PubMed](#)]
179. Tang, B.; Yong, X.; Xie, R.; Li, Q.W.; Yang, S.M. Vasoactive intestinal peptide receptor-based imaging and treatment of tumors. *Int. J. Oncol.* **2014**, *44*, 1023–1031. [[CrossRef](#)]
180. Emrarian, I.; Sadeghzadeh, N.; Abedi, S.M.; Abediankenari, S. New neurotensin analogue radiolabeled by ^{99m}Tc -technetium as a potential agent for tumor identification. *Chem. Biol. Drug Des.* **2018**, *91*, 304–313. [[CrossRef](#)]
181. Fanelli, R.; Chastel, A.; Previti, S.; Cavellier, F. Silicon-Containing Neurotensin Analogues as Radiopharmaceuticals for NTS1-Positive Tumors Imaging. *Bioconj. Chem.* **2020**, *31*, 2339–2349. [[CrossRef](#)]
182. Gao, F.; Sihver, W.; Bergmann, R.; Pietzsch, H.J. Synthesis, Characterization, and Initial Biological Evaluation of [^{99m}Tc]Tc-Tricarbonyl-labeled DPA- α -MSH Peptide Derivatives for Potential Melanoma Imaging. *ChemMedChem* **2018**, *13*, 1146–1158. [[CrossRef](#)] [[PubMed](#)]
183. Kobayashi, M.; Kato, T.; Washiyama, K.; Kawai, K. The pharmacological properties of 3-arm or 4-arm DOTA constructs for conjugation to α -melanocyte-stimulating hormone analogues for melanoma imaging. *PLoS ONE* **2019**, *14*, e0213397. [[CrossRef](#)]
184. Gao, F.; Sihver, W.; Bergmann, R.; Pietzsch, H.J. Radiochemical and radiopharmacological characterization of a ^{64}Cu -labeled α -MSH analog conjugated with different chelators. *J. Label. Compd. Radiopharm.* **2019**, *62*, 495–509. [[CrossRef](#)] [[PubMed](#)]
185. Qiao, Z.; Xu, J.; Gonzalez, R.; Miao, Y. Novel [^{99m}Tc]-Tricarbonyl-NOTA-Conjugated Lactam-Cyclized Alpha-MSH Peptide with Enhanced Melanoma Uptake and Reduced Renal Uptake. *Mol. Pharm.* **2020**, *17*, 3581–3588. [[CrossRef](#)] [[PubMed](#)]
186. Majkowska-Pilip, A.; Kozminski, P.; Wawrzynowska, A.; Gniazdowska, E. Application of Neurokinin-1 Receptor in Targeted Strategies for Glioma Treatment. *Molecules* **2018**, *23*, 2542. [[CrossRef](#)]
187. Zhang, H.; Kanduluru, A.K.; Desai, P.; Low, P.S. Synthesis and Evaluation of a Novel ^{64}Cu - and ^{67}Ga -Labeled Neurokinin 1 Receptor Antagonist for in Vivo Targeting of NK1R-Positive Tumor Xenografts. *Bioconj. Chem.* **2018**, *29*, 1319–1326. [[CrossRef](#)]
188. Lindner, S.; Fiedler, L.; Wängler, B.; Wängler, C. Design, synthesis and in vitro evaluation of heterobivalent peptidic radioligands targeting both GRP- and VPAC₁-Receptors concomitantly overexpressed on various malignancies—Is the concept feasible? *Eur. J. Med. Chem.* **2018**, *155*, 84–95. [[CrossRef](#)]
189. Kumar, P.; Tripathi, S.K.; Chen, C.P.; Wickstrom, E.; Thakur, M.L. Evaluating Ga-68 Peptide Conjugates for Targeting VPAC Receptors: Stability and Pharmacokinetics. *Mol. Imaging Biol.* **2019**, *21*, 130–139. [[CrossRef](#)]
190. Tripathi, S.K.; Kean, R.; Bongiorno, E.; Thakur, M.L. Targeting VPAC1 Receptors for Imaging Glioblastoma. *Mol. Imaging Biol.* **2020**, *22*, 293–302. [[CrossRef](#)]
191. Wester, H.J.; Schottelius, M. PSMA-Targeted Radiopharmaceuticals for Imaging and Therapy. *Semin. Nucl. Med.* **2019**, *49*, 302–312. [[CrossRef](#)]
192. Mhaweck-Fauceglia, P.; Zhang, S.; Terracciano, L.; Penetrante, R. Prostate-specific membrane antigen (PSMA) protein expression in normal and neoplastic tissues and its sensitivity and specificity in prostate adenocarcinoma: An immunohistochemical study using multiple tumour tissue microarray technique. *Histopathology* **2007**, *50*, 472–483. [[CrossRef](#)] [[PubMed](#)]
193. Wernicke, A.G.; Varma, S.; Greenwood, E.A.; Shin, S.J. Prostate-specific membrane antigen expression in tumor-associated vasculature of breast cancers. *APMIS* **2014**, *122*, 482–489. [[CrossRef](#)] [[PubMed](#)]
194. Haffner, M.C.; Kronberger, I.E.; Ross, J.S.; Bander, N.H. Prostate-specific membrane antigen expression in the neovasculature of gastric and colorectal cancers. *Hum. Pathol.* **2009**, *40*, 1754–1761. [[CrossRef](#)] [[PubMed](#)]
195. Schmidt, L.H.; Heitkötter, B.; Schulze, A.B.; Huss, S. Prostate specific membrane antigen (PSMA) expression in non-small cell lung cancer. *PLoS ONE* **2017**, *12*, e0186280. [[CrossRef](#)] [[PubMed](#)]

196. Spatz, S.; Tolkach, Y.; Jung, K.; Kristiansen, G. Comprehensive evaluation of prostate specific membrane antigen expression in the vasculature of renal tumors: Implications for imaging studies and prognostic role. *J. Urol.* **2018**, *199*, 370–377. [[CrossRef](#)]
197. Nomura, N.; Pastorino, S.; Jiang, P.; Kesari, S. Prostate specific membrane antigen (PSMA) expression in primary gliomas and breast cancer brain metastases. *Cancer Cell Int.* **2014**, *14*, 26. [[CrossRef](#)]
198. Tolkach, Y.; Goltz, D.; Kremer, A.; Kristiansen, G. Prostate-specific membrane antigen expression in hepatocellular carcinoma: Potential use for prognosis and diagnostic imaging. *Oncotarget* **2019**, *10*, 4149–4160. [[CrossRef](#)]
199. Eder, M.; Schäfer, M.; Bauder-Wuest, U.; Eisenhut, M. ⁶⁸Ga-complex lipophilicity and the targeting property of a urea-based PSMA inhibitor for PET imaging. *Bioconj. Chem.* **2012**, *23*, 688–697. [[CrossRef](#)]
200. Juillerat-Jeanneret, L.; Tafelmeyer, P.; Golshayan, D. Fibroblast activation protein- α in fibrogenic disorders and cancer: More than a prolyl-specific peptidase? *Expert Opin. Ther. Targets* **2017**, *21*, 977–991. [[CrossRef](#)]
201. Rettig, W.J.; Su, S.L.; Fortunato, S.R.; Old, L.J. Fibroblast activation protein: Purification, epitope mapping and induction by growth factors. *Int. J. Cancer* **1994**, *58*, 385–392. [[CrossRef](#)]
202. Kahounová, Z.; Kurfurstová, D.; Bouchal, J.; Souček, L. The fibroblast surface markers FAP, anti-fibroblast, and FSP are expressed by cells of epithelial origin and may be altered during epithelial-to-mesenchymal transition. *Cytom. A* **2017**, *93*, 941–951. [[CrossRef](#)] [[PubMed](#)]
203. Arnold, J.N.; Magiera, L.; Kraman, M.; Fearon, D.T. Tumoral Immune Suppression by Macrophages Expressing Fibroblast Activation Protein-Alpha and Heme Oxygenase-1. *Cancer Immunol. Res.* **2014**, *2*, 121–126. [[CrossRef](#)]
204. Busek, P.; Mateu, R.; Zubal, M.; Kotackova, L.; Sedo, A. Targeting fibroblast activation protein in cancer—Prospects and caveats. *Front. Biosci.* **2018**, *23*, 1933–1968.
205. Busek, P.; Vanickova, Z.; Hrabal, P.; Sedo, A. Increased tissue and circulating levels of dipeptidyl peptidase-IV enzymatic activity in patients with pancreatic ductal adenocarcinoma. *Pancreatol.* **2016**, *16*, 829–838. [[CrossRef](#)]
206. Shi, M.; Yu, D.H.; Chen, Y.; Zhu, M.H. Expression of fibroblast activation protein in human pancreatic adenocarcinoma and its clinicopathological significance. *World J. Gastroenterol.* **2012**, *18*, 840–846. [[CrossRef](#)] [[PubMed](#)]
207. Zou, B.; Liu, X.; Zhang, B.; Li, J. The Expression of FAP in Hepatocellular Carcinoma Cells is Induced by Hypoxia and Correlates with Poor Clinical Outcomes. *J. Cancer* **2018**, *9*, 3278–3286. [[CrossRef](#)]
208. Huang, Y.; Simms, A.E.; Mazur, A.; Kelly, T. Fibroblast activation protein- α promotes tumor growth and invasion of breast cancer cells through non-enzymatic functions. *Clin. Exp. Metastasis* **2011**, *28*, 567–579. [[CrossRef](#)]
209. Wikberg, M.L.; Edin, S.; Lundberg, I.V.; Palmqvist, R. High intratumoral expression of fibroblast activation protein (FAP) in colon cancer is associated with poorer patient prognosis. *Tumor Biol.* **2013**, *34*, 1013–1020. [[CrossRef](#)] [[PubMed](#)]
210. Mhawech-Fauceglia, P.; Yan, L.; Sharifian, M.; Lawrenson, K. Stromal Expression of Fibroblast Activation Protein Alpha (FAP) Predicts Platinum Resistance and Shorter Recurrence in patients with Epithelial Ovarian Cancer. *Cancer Microenviron.* **2015**, *8*, 23–31. [[CrossRef](#)]
211. Šimková, A.; Bušek, P.; Šedo, A.; Konvalinka, J. Molecular recognition of fibroblast activation protein for diagnostic and therapeutic applications. *Biochim. Biophys. Acta Proteins Proteomics* **2020**, *1868*, 140409. [[CrossRef](#)]
212. Lindner, T.; Loktev, A.; Altmann, A.; Haberkorn, U. Development of Quinoline-Based Theranostic Ligands for the Targeting of Fibroblast Activation Protein. *J. Nucl. Med.* **2018**, *59*, 1415–1422. [[CrossRef](#)] [[PubMed](#)]
213. Loktev, A.; Lindner, T.; Burger, E.M.; Haberkorn, U. Development of Fibroblast Activation Protein-Targeted Radiotracers with Improved Tumor Retention. *J. Nucl. Med.* **2019**, *60*, 1421–1429. [[CrossRef](#)]
214. Kulkarni, M.; Hughes, S.; Mallia, A.; Cook, G.J.R. The management impact of ⁶⁸Ga-tris(hydroxypyridinone) prostate-specific membrane antigen (⁶⁸Ga-THP-PSMA) PET-CT imaging for high-risk and biochemically recurrent prostate cancer. *Eur. J. Nucl. Med. Mol. Imaging* **2020**, *47*, 674–686. [[CrossRef](#)]
215. Mosayebnia, M.; Hajimahdi, Z.; Beiki, D.; Shahhosseini, S. Design, synthesis, radiolabeling and biological evaluation of new urea-based peptides targeting prostate specific membrane antigen. *Bioorg. Chem.* **2020**, *99*, 103743. [[CrossRef](#)]
216. Dos Santos, J.C.; Beijer, B.; Bauder-Wuerst, U.; Mier, W. Development of Novel PSMA Ligands for Imaging and Therapy with Copper Isotopes. *J. Nucl. Med.* **2020**, *61*, 70–79. [[CrossRef](#)]
217. Kunikowska, J.; Kulinski, R.; Muylle, K.; Koziara, H.; Krolicki, L. ⁶⁸Ga-Prostate-Specific Membrane Antigen-11 PET/CT A New Imaging Option for Recurrent Glioblastoma Multiforme? *Clin. Nucl. Med.* **2020**, *45*, 11–18. [[CrossRef](#)] [[PubMed](#)]
218. Ghiani, S.; Hawala, I.; Szikra, D.; Maiocchi, A. Synthesis, radiolabeling, and pre-clinical evaluation of [⁴⁴Sc]Sc-AAZTA conjugate PSMA inhibitor, a new tracer for high-efficiency imaging of prostate cancer. *Eur. J. Nucl. Med. Mol. Imaging* **2021**. [[CrossRef](#)] [[PubMed](#)]
219. Loktev, A.; Lindner, T.; Mier, W.; Haberkorn, U. A Tumor-Imaging Method Targeting Cancer-Associated Fibroblasts. *J. Nucl. Med.* **2018**, *59*, 1423–1429. [[CrossRef](#)]
220. Giesel, F.L.; Kratochwil, C.; Lindner, T.; Haberkorn, U. ⁶⁸Ga-FAPI PET/CT: Biodistribution and Preliminary Dosimetry Estimate of 2 DOTA-Containing FAP-Targeting Agents in Patients with Various Cancers. *J. Nucl. Med.* **2019**, *60*, 386–392. [[CrossRef](#)] [[PubMed](#)]
221. Syed, M.; Flechsig, P.; Liermann, J.; Adeberg, S. Fibroblast activation protein inhibitor (FAPI) PET for diagnostics and advanced targeted radiotherapy in head and neck cancers. *Eur. J. Nucl. Med. Mol. Imaging* **2020**, *47*, 2836–2845. [[CrossRef](#)] [[PubMed](#)]
222. Kratochwil, C.; Flechsig, P.; Lindner, T.; Giesel, F.L. ⁶⁸Ga-FAPI PET/CT: Tracer Uptake in 28 Different Kinds of Cancer. *J. Nucl. Med.* **2019**, *60*, 801–805. [[CrossRef](#)]

223. Röhrich, M.; Loktev, A.; Wefers, A.K.; Haberkorn, U. IDH-wildtype glioblastomas and grade III/IV IDH-mutant gliomas show elevated tracer uptake in fibroblast activation protein-specific PET/CT. *Eur. J. Nucl. Med. Mol. Imaging* **2019**, *46*, 2569–2580. [[CrossRef](#)] [[PubMed](#)]
224. Watabe, T.; Liu, Y.; Nakashima, K.K.; Hatazawa, J. Theranostics targeting fibroblast activation protein in the tumor stroma: ^{64}Cu and ^{225}Ac labelled FAPI-04 in pancreatic cancer xenograft mouse models. *J. Nucl. Med.* **2019**. [[CrossRef](#)] [[PubMed](#)]
225. Shi, X.; Xing, H.; Yang, X.; Li, X. Fibroblast imaging of hepatic carcinoma with ^{68}Ga -FAPI-04 PET/CT: A pilot study in patients with suspected hepatic nodules. *Eur. J. Nucl. Med. Mol. Imaging* **2020**, *48*, 196–203. [[CrossRef](#)]
226. Meyer, C.; Dahlbom, M.; Lindner, T.; Calais, J. Radiation Dosimetry and Biodistribution of ^{68}Ga -FAPI-46 PET Imaging in Cancer Patients. *J. Nucl. Med.* **2020**, *61*, 1171–1177. [[CrossRef](#)] [[PubMed](#)]
227. Windisch, P.; Röhrich, M.; Regnery, S.; Adeberg, S. Fibroblast Activation Protein (FAP) specific PET for advanced target volume delineation in glioblastoma. *Radiother. Oncol.* **2020**, *150*, 159–163. [[CrossRef](#)] [[PubMed](#)]
228. Chen, H.; Zhao, L.; Ruan, D.; Wu, H. Usefulness of ^{68}Ga [Ga-DOTA-FAPI-04 PET/CT in patients presenting with inconclusive ^{18}F]FDG PET/CT findings. *Eur. J. Nucl. Med. Mol. Imaging* **2020**, *48*, 73–86. [[CrossRef](#)]
229. Chen, H.; Pang, Y.; Wu, J.; Wu, H. Comparison of ^{68}Ga [Ga-DOTA-FAPI-04 and ^{18}F]FDG PET/CT for the diagnosis of primary and metastatic lesions in patients with various types of cancer. *Eur. J. Nucl. Med. Mol. Imaging* **2020**, *47*, 1820–1832. [[CrossRef](#)] [[PubMed](#)]
230. Lindner, T.; Altman, A.; Krämer, S.; Haberkorn, U. Design and Development of $^{99\text{m}}\text{Tc}$ -Labeled FAPI Tracers for SPECT Imaging and ^{188}Re Therapy. *J. Nucl. Med.* **2020**, *61*, 1507–1513. [[CrossRef](#)]
231. Petrova, V.; Annicchiarico-Petruzzelli, M.; Melino, G.; Amelio, I. The hypoxic tumour microenvironment. *Oncogenesis* **2018**, *7*, 10. [[CrossRef](#)]
232. Ruan, Q.; Zhang, X.; Gan, Q.; Fang, S.; Zhang, J. Preparation of two $^{99\text{m}}\text{Tc}(\text{CO})_3$ labelled complexes with a 4-nitroimidazole isocyanide at different temperatures for molecular imaging of tumor hypoxia. *J. Radioanal. Nucl. Chem.* **2020**, *323*, 851–859. [[CrossRef](#)]
233. Ruan, Q.; Zhang, X.; Gan, Q.; Fang, S.; Zhang, J. Synthesis and evaluation of $^{99\text{m}}\text{TcN}^{2+}$ core and $^{99\text{m}}\text{TcO}^{3+}$ core labeled complexes with 4-nitroimidazole xanthate derivative for tumor hypoxia imaging. *Bioorg. Med. Chem. Lett.* **2020**, *30*, 127582. [[CrossRef](#)]
234. Luo, Z.; Zhu, H.; Lin, X.; Chu, T.; Yang, Z. Synthesis and radiolabeling of ^{64}Cu -labeled 2-nitroimidazole derivative ^{64}Cu -BMS2P2 for hypoxia imaging. *Bioorg. Med. Chem. Lett.* **2016**, *26*, 1397–1400. [[CrossRef](#)]
235. Seelam, S.R.; Lee, J.Y.; Lee, Y.S.; Jeong, J.M. Development of ^{68}Ga -labeled multivalent nitroimidazole derivatives for hypoxia imaging. *Bioorg. Med. Chem.* **2015**, *23*, 7743–7750. [[CrossRef](#)]
236. Lau, J.; Lin, K.S.; Bénard, F. Past, Present, and Future: Development of Theranostic Agents Targeting Carbonic Anhydrase IX. *Theranostics* **2017**, *7*, 4322–4339. [[CrossRef](#)]
237. Van Dijk, L.K.; Boerman, O.C.; Kaanders, J.H.A.M.; Bussink, J. Epidermal growth factor receptor imaging in human head and neck cancer xenografts. *Acta Oncol.* **2015**, *54*, 1263–1267. [[CrossRef](#)] [[PubMed](#)]
238. Obacz, J.; Pastorekova, S.; Vojtesek, B.; Hrstka, R. Cross-talk between HIF and p53 as mediators of molecular responses to physiological and genotoxic stresses. *Mol. Cancer* **2013**, *12*, 93. [[CrossRef](#)] [[PubMed](#)]
239. Mikulová, M.B.; Kružlicová, D.; Pecher, D.; Supuran, C.T.; Mikuš, P. Synthetic strategies and computational inhibition activity study for triazinyl-substituted benzenesulfonamide conjugates with polar and hydrophobic amino acids as inhibitors of carbonic anhydrases. *Int. J. Mol. Sci.* **2020**, *21*, 3661. [[CrossRef](#)] [[PubMed](#)]
240. Iikuni, S.; Ono, M.; Watanabe, H.; Saji, H. Cancer radiotheranostics targeting carbonic anhydrase-IX with ^{111}In - and ^{90}Y -labeled ureidosulfonamide scaffold for SPECT imaging and radionuclide-based therapy. *Theranostics* **2018**, *8*, 2992–3006. [[CrossRef](#)] [[PubMed](#)]
241. Nakai, M.; Pan, J.; Lin, K.S.; Storr, T. Evaluation of $^{99\text{m}}\text{Tc}$ -sulfonamide and sulfocoumarin derivatives for imaging carbonic anhydrase IX expression. *J. Inorg. Biochem.* **2018**, *185*, 63–70. [[CrossRef](#)] [[PubMed](#)]
242. Iikuni, S.; Tanimura, K.; Watanabe, H.; Shimizu, Y.; Saji, H.; Ono, M. Development of the $^{99\text{m}}\text{Tc}$ -Hydroxamamide Complex as a Probe Targeting Carbonic Anhydrase IX. *Mol. Pharm.* **2019**, *16*, 1489–1497. [[CrossRef](#)] [[PubMed](#)]
243. Iikuni, S.; Okada, Y.; Shimizu, Y.; Watanabe, H.; Ono, M. Synthesis and evaluation of indium-111-labeled imidazothiadiazole sulfonamide derivative for single photon emission computed tomography imaging targeting carbonic anhydrase-IX. *Bioorg. Med. Chem. Lett.* **2020**, *30*, 127255. [[CrossRef](#)] [[PubMed](#)]